A Review of the Characteristics of Tornadic Wind Fields through Observations and Simulations

Ryan Honerkamp^a, Guirong Yan^b, and Jeffrey C. Snyder^c

^a Department of Civil, Architectural and Environmental Engineering, Missouri University of Science and Technology, Rolla, MO 65409, rh7v7@umsystem.edu

^b Department of Civil, Architectural and Environmental Engineering, Missouri University of Science and Technology, Rolla, MO 65409, yang@umsystem.edu

^c NOAA/OAR/National Severe Storms Laboratory, Norman, OK 73072, jeffrey.snyder@noaa.gov

ABSTRACT

Tornadoes are violently rotating columns of air that may be produced by convective clouds and storms, and they can produce substantial property damage, injuries, and deaths. To mitigate these losses and encourage accurate modeling and research in the field of civil engineering, with the goal of improving civil structure design, a comprehensive review of field measurements, lab simulations, and computational fluid dynamics (CFD) simulations of tornadoes is conducted. From this review, several tornadoes are examined and their characteristics presented. Specifically, characteristics of these tornadoes are provided in the following form: velocity of the wind field, pressure distribution associated with the wind field, tornado core radius, and flow structure (i.e., single vortex versus multiple vortices; for single vortex, one-celled versus two-celled). In addition, the driving forces behind tornadoes and the relationships between damage and reported intensity are examined, and the physical and numerical simulation of tornadoes conducted in civil engineering are reviewed. This paper is intended to provide a baseline review so that more accurate simulations of tornadic wind fields in civil engineering research can be made by providing some field-measured data from the meteorology community. This will benefit individual safety, community resilience and awareness, and simulation accuracy for future research.

Keyword: Review, Tornado Dynamics, Tornadic Wind Field, Civil Engineering, Meteorology

1. INTRODUCTION

According to the American Meteorological Society, a tornado is "a rotating column of air, in contact with the surface, pendant from a cumuliform cloud, and often visible as a funnel cloud and/or circulating debris/dust at the ground" [1] (see Fig. 1). Tornadoes are one of the most violent natural hazards; wind speeds exceeding 130 m s⁻¹ (268 mph) have been measured by radar [2, 3, 4, 5]. Approximately 1200 tornadoes occur in the United States each year based on statistics from the National Oceanic and Atmospheric Administration (NOAA) [6,7], resulting in substantial amounts of property damage and significant numbers of injuries and fatalities each year [8]. During the period of 1949-2006, the average annual economic loss due to tornadoes was about \$1 billion [9,10,11]. Annually, tornadoes cause an average of ~90 fatalities and ~1500 injuries [12], though some years are much worse than others [13]. In 2011, the tornado-induced property loss exceeded \$20 billion, and 550 people were killed [14,15]. In particular, the Joplin, MO, tornado of 22 May 2011, which was rated EF-5 (the highest rating) on the Enhanced Fujita scale, resulted in 1150 injuries, 158 deaths, and \$2.8 billion of property damage [16,17]. Many more people may be killed if high-intensity tornadoes strike metropolitan areas; according to one study [18], 43,800 may be

killed in a Chicago, IL setting, 14,300 in a St. Louis, MO setting, and 22,100 in a Dallas-Fort Worth, TX setting. Regardless of civilization's advances in meteorology and engineering, tornadoes remain a threat that pose a continuing risk for catastrophic loss of life and property.



Fig. 1 A tornado that occurred in the Texas panhandle on 28 March 2007. (Photo courtesy of Jeffrey Snyder)

There are several reasons for the high tornado-induced life and property losses. First, the lead time for most tornadoes is relatively short compared to that for other meteorological phenomena that produce substantial loss; the average tornado warning lead time, for tornadoes warned in advance, is between 15 and 20 minutes [19], much lower than the usual lead time for some other meteorological phenomena that can produce similarly large losses. For example, tropical cyclones may develop far from land and be tracked for days and weeks before they directly impact land and population centers. Tropical cyclones tend to move more slowly than do tornadoes (e.g., often at a maximum speed of 10 m/s [20, 21]), tend to be much larger (on the order of 1000 km), last much longer (more days and weeks versus seconds and minutes), and tend to be more readily observed with remote sensing equipment, all factors of which tend to increase their predictability relative to that of tornadoes. Because of the lower lead time for tornadoes, communities do not have sufficient time to mitigate losses to buildings and properties if actions are taken only after an impact from a specific tornado is expected or after a tornado warning is issued.

Second, tornadoes can produce extremely high wind speeds, sometimes exceeding 130 m/s at tornado core radius (i.e., the radius where the maximum tangential velocity is observed), and produce very high atmospheric pressure drops (i.e., negative pressure perturbations) at tornado center. With a high wind speed and large atmospheric pressure drop, very large wind pressure (including pressure and suction) will be exerted on civil structures, damaging structural/nonstructural components or even destroying the entire civil structure. The high wind

speed can produce and subsequently loft debris from damaged buildings, vehicles, or other objects previously on the ground. Lofted debris can become missiles that impact other structures and generate more wind-borne debris.

In addition to the limited lead time and violent nature of the winds in tornadoes, a third factor contributing to the large loss figures in tornadoes is our current limited understanding of the effects of tornadic winds on civil structures. One of the primary difficulties in this regard is in collecting observations with sufficient resolution to capture the detailed flow structure and evolution of tornadoes, regardless of tornado size. Collecting in-situ measurements of tornadic winds around civil structures (i.e., within ~10 m of the ground) is extremely difficult owing to the limited predictability of tornadoes (which makes placing observing equipment near and within a tornado extraordinarily difficult) and to the inherent dangers (to instruments and the humans deploying the instruments) associated with placing instrumentation near buildings immediately ahead of a tornado. Because tornadoes can be so violent, are often relatively short lived with lifetimes on the order of 1-10 minutes, and tend to have less predictable paths and life-cycles [22,23,24] relative to the parent thunderstorm (and other phenomena such as tropical cyclones), even the most advanced remote sensing technology (e.g., high-resolution, rapid-scan mobile radars) has extreme difficulties sampling near buildings. Owing to beam broadening, ground clutter contamination, and terrain irregularities, data from radars is often limited to elevations non-trivially [i.e., O(10-100 m)] above building or structure height.

A report detailing a violent tornado that affected Joplin, MO, on 22 May 2011 stated that, among all of the fatalities during this event, 84% were related to building failure [25]. Building failures can be caused by any of the following: 1) large positive pressure due to high wind speeds; 2) large negative (suction) pressure owing to the pressure drop at the tornado's center; 3) impacts from wind-borne debris; and 4) aerodynamic instability induced by flow within the tornado. The relative importance of each of these depends, in part at least, on the distance of the building from the center of the tornado. For example, close to tornado center, a roof may be lifted due to a high atmospheric pressure drop and strong vertical wind velocities; away from the tornado center, but close to the tornado core radius, the building envelope may be breached due to high quasi-horizontal wind speeds. Near the tornado's core region, the building may be damaged by the impact of wind-borne debris, which can severely reduce building integrity. Aerodynamic instability not only depends on the turbulent nature of the tornado but also on the dynamic characteristics of the building itself.

To reduce or prevent structural failure and mitigate associated injuries and fatalities, building design codes need to be improved. Such an improvement requires an in-depth understanding of tornadic wind fields and their effects on civil structures. Although civil engineering researchers have been investigating tornadic wind effects through theoretical analyses, testing in laboratory tornado simulators, and CFD simulations [e.g., 26, 27, 28, 29, 30, 31, 32, 33, 34, 35, 36, 37], validation using field-measured data is extremely limited. The present authors intend the information presented herein to help civil engineers and researchers improve the accuracy of simulated tornadic wind fields and determine tornadic wind loads more properly. Specifically, this paper serves as a reference for civil engineers and researchers to compare their data, be it from physical or numerical simulation, with that of meteorological results, thus estimating more realistic wind loadings on structures.

The remainder of this paper is structured such that each section describes the current understanding of each of the following topics or processes: 1) tornadogenesis, 2) wind velocity fields in tornadoes, 3) velocity measurements near the ground, 4) pressure fields in tornadoes, 5) tornado core radius, 6) flow structure of tornadoes, 7) relationship between damage, debris, and radar-measured velocity data, 8) tornadic wind load calculation specified in ASCE7-16, 9) characterization of tornadic wind fields using CFD simulations or laboratory tornado simulator from the field of meteorology, 10) characterization of tornadic wind fields using CFD simulations or laboratory tornado simulator from the field of civil engineering.

2. TORNADOGENESIS

Owing to the desire for a holistic understanding of processes in the natural world and, on a more practical level, the desire to increase warning lead time, the process by which tornadoes develop (i.e., tornadogenesis) has been the topic of much research. The relevant processes and sources of vorticity associated with tornadoes may be different in different tornadoes, although a sort of informal and somewhat arbitrary classification of tornadoes does exist in the meteorological community. These "types" of tornadoes include so-called landspout and waterspout tornadoes (which are generally the result of stretching of a misoscale vertical vorticity maximum beneath and within a growing cumulus or cumulus congestus cloud), quasi-linear convective system (QLCS) tornadoes (which tend to occur along the leading edge of outflow associated with QLCSs), and tornadoes associated with the mesocyclone of a supercell. For the sake of this discussion, socalled "gustnadoes" and "dust devils" are not considered to be tornadoes because their rotation is often not connected to and driven by a parent convective cloud. Although there may be differences in the underlying processes driving each of the aforementioned "types" of tornado, the fundamental structure of each "type" may be quite similar, at least in that part of the tornado near the ground. Since most strong (i.e., EF2-3) and violent (i.e., EF4-5) tornadoes are associated with mesocyclones within supercells and since such tornadoes produce the vast majority of damage and casualties, we will focus primarily on this "type" of tornado.

Popular methods used to study tornadoes have included the development of mathematics-based theory, the use of high-resolution numerical models, and the collection and analysis of observational data. Despite substantial past work, the details of tornadogenesis are still quite unknown. Results from previous field projects, including the Verification of the Origins of Rotation in Thunderstorms (VORTEX) project and its successor (VORTEX2), have shown that many tornadic supercells look quite similar to non-tornadic supercells at heights exceeding ~1 km above ground level (AGL). The rotation associated with the mesocyclone (the rotating updraft of a supercell) is generally understood to be the result of the tilting of horizontally aligned vorticity associated with environmental vertical wind shear into the vertical and the subsequent stretching of the resultant vertical vorticity within the buoyant updraft. The process by which tornadoes develop within mesocyclones, however, is likely not directly driven by the tilting and stretching of streamwise vorticity associated with environmental wind shear. Tilting of horizontal vorticity in the vertical by itself cannot create a tornado because that process creates vertical vorticity above the ground, not at the ground [38].

Results from VORTEX [39] and additional field projects since that time [40] have shown that the thermodynamic character of the rear-flank downdrafts (RFDs) in tornadic and nontornadic

supercells are, on average, different. In tornadic supercells, the air in the RFD tends to be only marginally cooler (if not warmer) than the ambient, pre-storm air. In contrast, the air in the RFD of non-tornadic supercells tends to be considerably colder than the pre-storm air.

A highly-idealized and simple tornado model is examined in Markowski et al. (2014) [41], as illustrated in Fig. 2 [42], which highlights the role of a downdraft in transporting vorticity to very near the ground. Other studies indicate that vorticity in parcels that comprise a tornado can be created via baroclinic generation above the near-ground layer, and crosswise-streamwise exchange can occur near the ground as the air is pulled inward towards the low-level mesocyclone. In addition, there are indications that, at least in some tornadoes, the presence of friction between the ground and atmosphere can affect tornadogenesis [43, 44]. Regardless of the source(s) of vorticity, rapid vertical acceleration associated with a strong upward-directed vertical perturbation pressure gradient force within the low-level mesocyclone turns and stretches such parcels rapidly upward. The exact source of the vorticity and the dominant means by which parcels obtain that vorticity is still an area of active research.

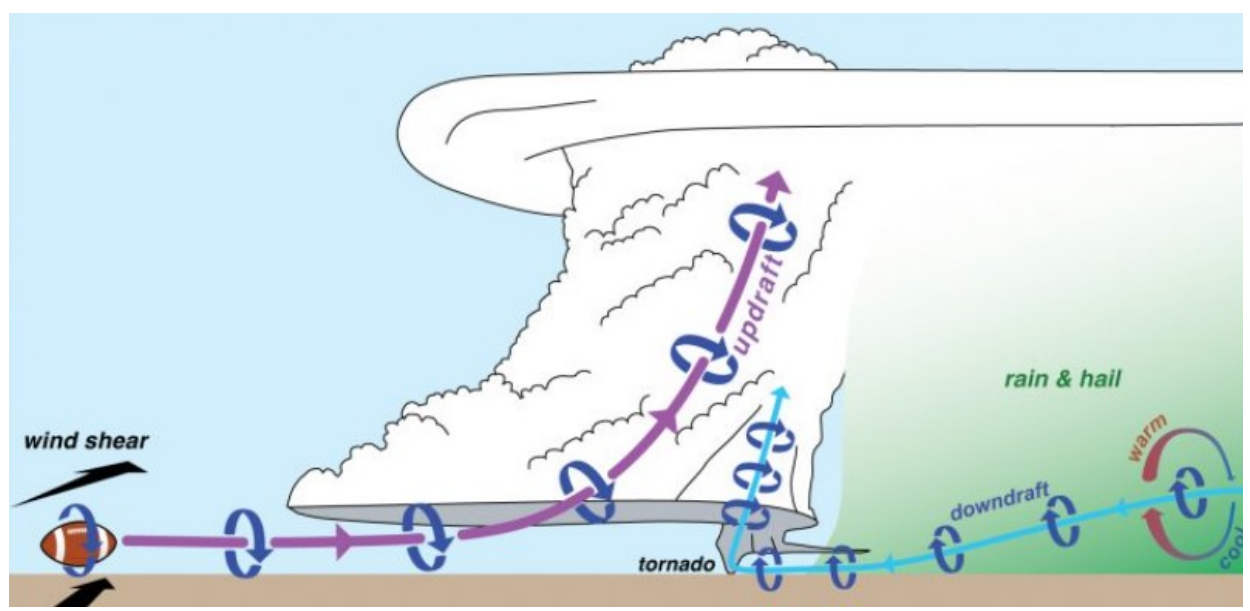


Fig. 2: A simple illustration of the origins of vertical vorticity in a supercell's updraft and in a tornado. Courtesy of Paul Markowski. Used with permission. [42]

3. WIND VELOCITY FIELDS IN TORNADOES

Weather radars, both mobile and fixed-site, and in-situ instruments have been used to estimate and/or measure winds within tornadoes [e.g., 45, 46, 47, 48, 49, 50, 51, 52, 53, 54, 55, 56]. Although fixed-site radars and quasi-permanent weather observation sites [57] have serendipitously measured winds in tornadoes, mobile radars have been extremely valuable tools for observing and studying tornadoes because they have been able to be placed in close proximity to tornado-producing storms to maximize the probability of collecting high-resolution, nearground data within tornadoes. Even still, it is extremely important to keep in mind that weather radars do not measure winds directly. Rather, they measure objects that may or may not be moving in directions and speeds similar to the local air motion, which means that the radar-estimated

velocity may not reflect the real wind speed and direction. In addition, measurements are averages over some volume that is, at best, on the order of 10⁴ m³ and often at least several orders of magnitude larger, so these are far from point measurements that in-situ instruments may collect. Despite substantial efforts, though, only a small handful of tornadoes have been directly sampled by a purpose-built in-situ instrument [48, 58, 59].

In a tornado-centric reference frame, a cylindrical decomposition of the three-dimensional wind field is often used, wherein the winds are described by the tangential (Vt), radial (Vr), and vertical (Vw) components [53,60]. Vt describes the "swirling" (i.e., azimuthal) winds rotating around the central axis of the tornado, Vr describes the winds moving inward or outward (i.e., towards or away) from the center of the tornado, and Vw describes the vertical component of air motion. (Care should be taken not to confuse this radial velocity component Vr with the velocity of the same name often used to describe the component measured by weather radars, in which the radial direction is relative to the radar not to the center of the tornado). Although the relationships between the velocity components and environmental factors (e.g., surface roughness) are subject to further study, researchers in both the meteorology and civil engineering fields require "real-life" data to assess and validate numerical models. This section presents the characteristics of velocities in several noteworthy, observed/well documented tornadoes.

An intense, F4 tornado occurred in Spencer, SD, on 30 May 1998 (subsequently referred to as the "Spencer tornado") [50,51]. This tornado was well documented by a nearby, high-resolution mobile radar. The azimuthally averaged Vt profiles as a function of the radial distance from the center of the tornado were extracted from the radar-measured velocity data and are presented in Fig. 3 [61,62]. From Fig. 3, at each altitude, the velocity increases rapidly from tornado center to a maximum at the core radius and then decreases gradually in the far field. For a one-celled tornado (in contrast to a two-celled or multi-vortex tornado), the area within the core radius is described by solid body rotation and characterized by approximately constant vorticity, such that the maximum Vt is observed at the core radius. Fig. 4 provides the maximum Vt measurements at each altitude [51]. In Figs. 3 and 4, the maximum, tornado-relative Vt is shown to be 81 m/s and 97 m/s, respectively. The values presented in Fig. 3 are time averaged, while the values in Fig. 4 are instantaneous.

The translation speed refers to how fast the tornado vortex moves along its path. It has generally been estimated using radar measurements, photographic evidence, or video. The translation speed of the Spencer tornado was ~15 m/s. The translation of the tornado can create asymmetries in the wind field even for an otherwise axisymmetric tornado. Fig. 5 illustrates how the translation speed affects the two horizontal wind components within the vortex. In Fig. 5, the length of the arrow represents the magnitude of the velocity component. The non-zero translation speed modifies the magnitudes of the ground-relative horizontal velocity components in tornadoes that are otherwise (i.e., if stationary) axisymmetric (Fig. 5a). To be specific, as shown in Fig. 5b, with the current assumptions in this illustration, the non-zero translation speed adds to the Vt on the right side (relative to the direction of translation) of the tornado and subtracts from it on the left side of the tornado. The translating speed adds to the Vr component on the rear side of the tornado and subtracts from it on the front side. In the Spencer tornado, the measured wind speeds on opposite sides of the vortex differed by ~30 m/s, which induced higher damage on the right side of the tornado path as opposed to the left [51]. This further demonstrates the asymmetric characteristics

of some tornadoes. The translating speeds of a small set of documented tornadoes are listed in Table 1. It is noted that the method for determining these values varies from source to source (i.e. averaged, instantaneous, etc.) and therefore these values serve only as a qualitative example of translating speeds. The translating speeds are typically on the order of 10 m/s though vary widely both during the lifetime of a tornado and from tornado to tornado.

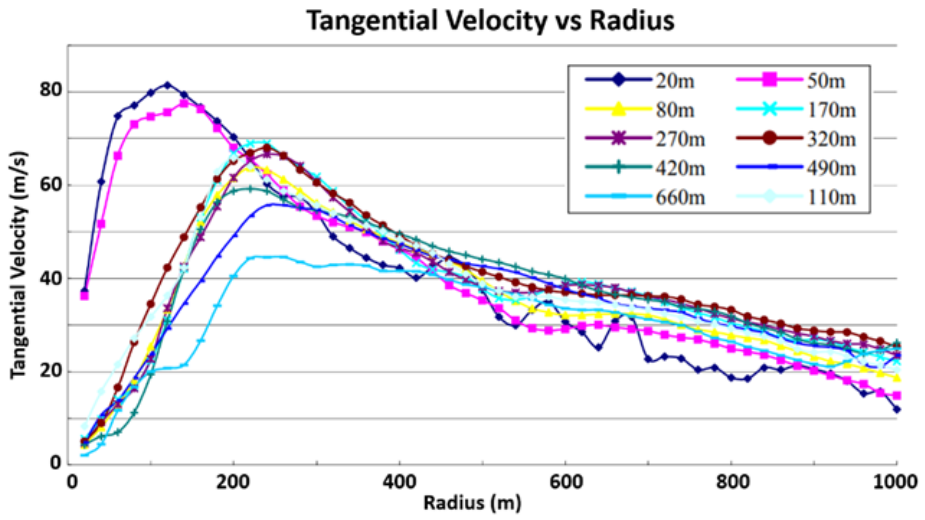


Fig. 3: Vt profile of the Spencer tornado with respect to the radial distance (from tornado center) for different altitudes. [61, 62]

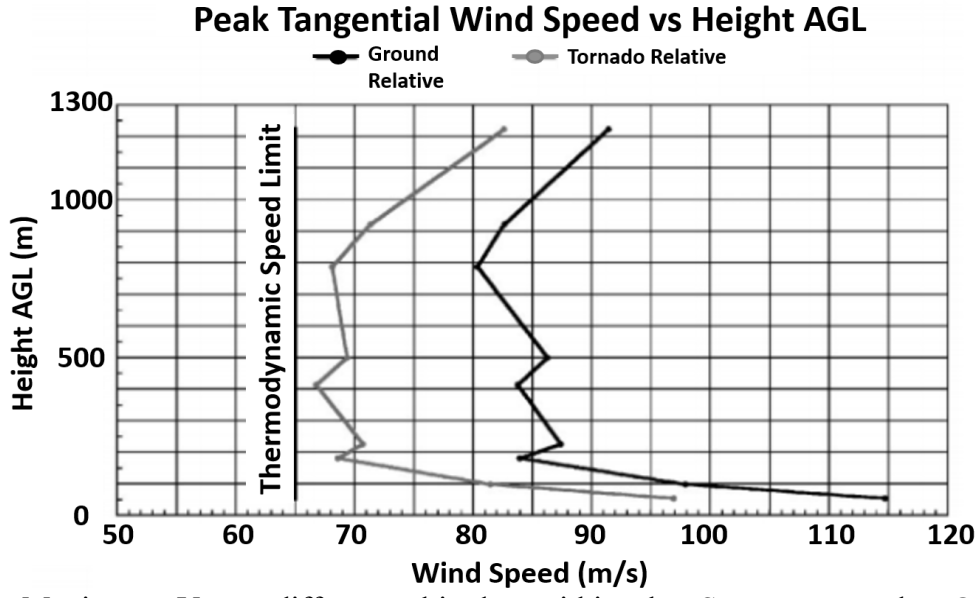


Fig. 4: Maximum Vt at different altitudes within the Spencer tornado. © American Meteorological Society. Used with permission. [51]

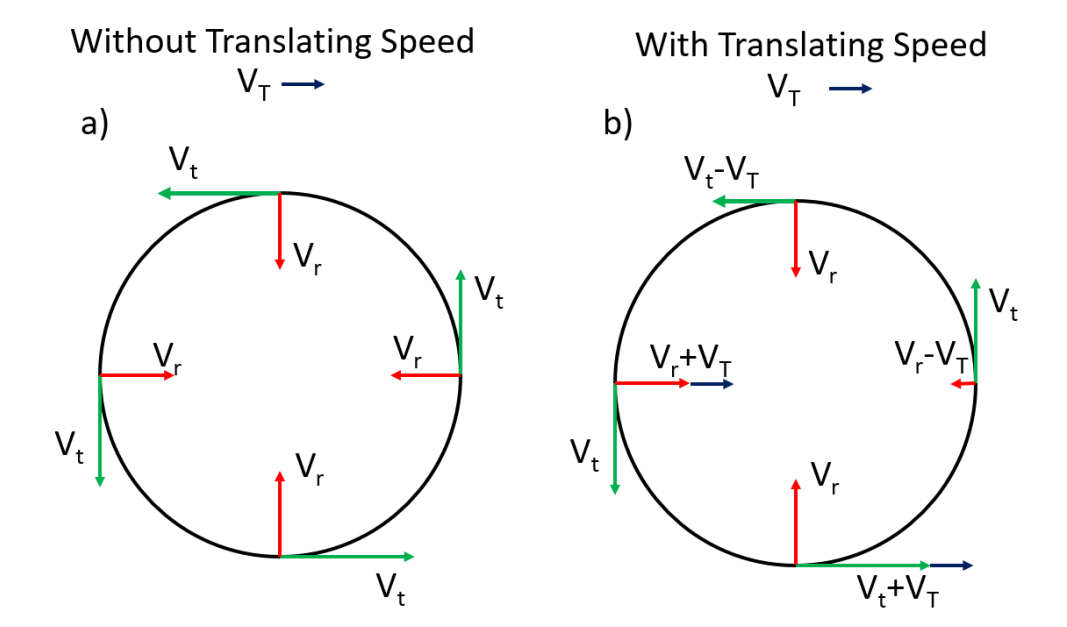


Fig. 5: (a) The velocity vectors for Vt and Vr and (b) the net effect of a non-zero translating speed (V_T) on Vt and Vr of an idealized, axisymmetric vortex.

Table 1: Translating Speed of Tornadoes from Multiple Sources. The values serve as a qualitative example of translating speeds from a small sample of tornadoes.

| Tornado | Translating | Fujita Rating |
|--|-------------|--------------------|
| | Speed | J 5 |
| Bridgecreek/Moore, OK on 3 May 1999 [18] | 9 m/s | F-5 |
| Mulhall, OK on 4 May 1999 [45] | 13.5 m/s | F-4 |
| Mullinville, KS on 7 May 2002 [59] | 5.7 m/s | F-3 |
| Stratford, TX on 15 May 2003 [59] | 15 m/s | F-3 |
| Manchester, SD on 24 June 2003 (Case 1) [59] | 9.4 m/s | F-4 |
| Manchester, SD on 24 June 2003 (Case 2) [59] | 2.3 m/s | F-4 |
| Webb, IA on 11 June 2004 [59] | 7.7 m/s | F-3 |
| Broken Bow, OK on 10 May 2008 [59] | 12 m/s | No Rating Provided |
| Quinter, KS on 23 May 2008 [58] | 20 m/s | No Rating Provided |
| Tipton, KS on 29 May 2008 [59] | 14.6 m/s | EF-1 |
| Beloit, KS on 29 May 2008 [59] | 5 m/s | EF-0 |
| Joplin, MO on 22 May 2011 [63] | 13 m/s | EF-5 |

Another F4 tornado occurred in Mulhall, OK, on 4 May 1999 (subsequently referred to as the "Mulhall tornado"). Profiles of Vt along the radial distance of the tornado are shown in Fig. 6 [64]. The maximum Vt in these data was found to be 84 m/s (see Fig. 6a). When Vt in the Mulhall tornado is normalized to the maximum Vt and tornado core radius, the values follow the Rankine vortex curve well for all heights (see Fig. 6b), especially inside the tornado core.

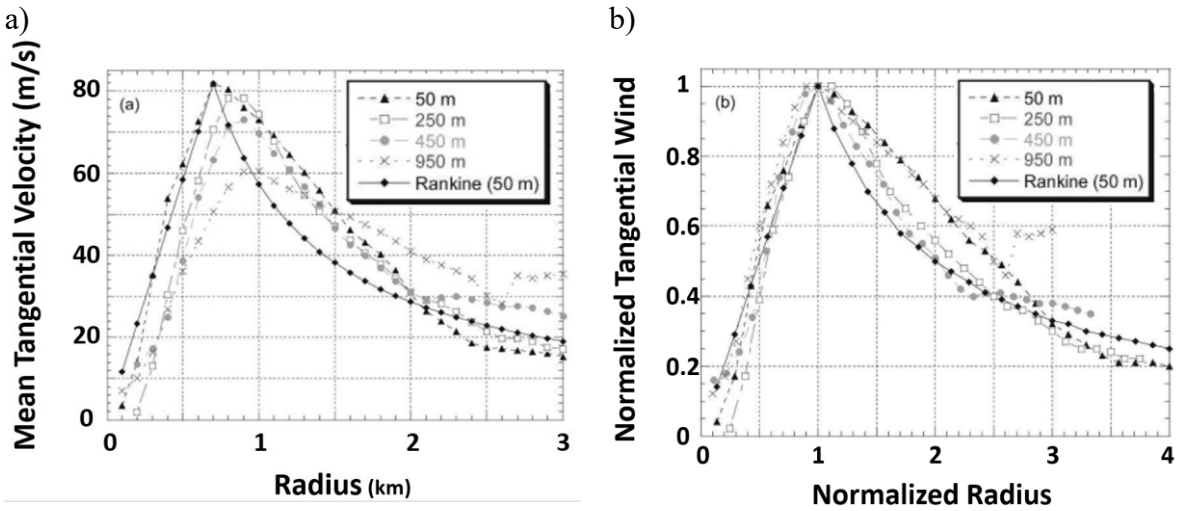


Fig. 6: (a) Dimensional and (b) normalized mean (i.e., azimuthally averaged) Vt profile for the Mulhall tornado at different altitudes. © American Meteorological Society. Used with permission [64].

Wurman et al (2013) describe observations of an EF-2 tornado that occurred in Goshen County, WY, on 5 June 2009 (subsequently referred to as the "Goshen tornado") [48]. The maximum Vt of the Goshen tornado was found to be ~40 m/s, as shown in Fig. 7. The Vt followed the characteristic curve of increasing from the center to the core radius and decreasing in the far field outside the core radius. A similar pattern was reported by Bluestein et al. (2003) using GBVTD-derived winds collected by a high-resolution mobile radar of a tornado near Bassett, NE, in 1999 [65].

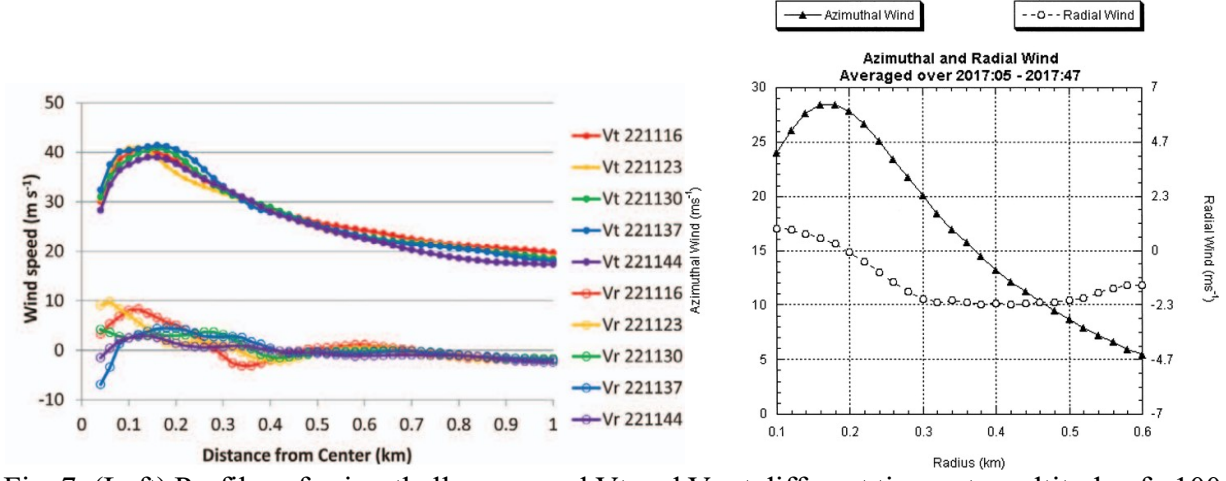


Fig. 7: (Left) Profiles of azimuthally averaged Vt and Vr at different times at an altitude of \sim 100 m above ground in the Goshen tornado [48]. (Right) Azimuthally averaged radial profiles of Vt and Vr retrieved by the Bassett tornado [65]. © American Meteorological Society. Used with permission.

Kosiba et al (2014) studied a tornado that passed over the Hong Kong International Airport, using LIDAR, surface weather stations, and Terminal Doppler Weather Radar (TDWR) [52]. From the

collected data, plots of the velocity, directions, and tornado core radius were created. Additionally, these data were compared to a Rankine vortex model to determine the structure of the vortex. The best fit Rankine vortex model was achieved by using a decay exponent equal to one in the general parameterized equation [66,67], which according to Kosiba et al (2014), "may suggest that frictionally induced inflow near the surface transported higher angular momentum inwards," which suggests that as the friction from the surface increases, the Vr decreases. This vortex demonstrated a decrease in Vr with time as the Vt and angular momentum increased. This suggests an interplay between the different components of the velocity, depending upon the location relative to tornado center.

4. VELOCITY MEASUREMENTS NEAR THE GROUND

The information presented previously focuses primarily on high altitude measurements. When attempting to collect measurements of tornadoes very near the ground, there are some methods that available, such as use of Doppler LIDAR technology, but this technology has difficulty collecting data when precipitation, debris, or other opaque materials are present [3]. Researchers have attempted to measure or predict near-ground wind speeds using alternative means, including with the use of mobile Doppler radars [68], physical laboratory simulator experimentation and mathematical calculation [69,70,71,72,73], and the analysis of tree-fall patterns associated with tornado damage in forested areas [74,75,76].

Kosiba and Wurman (2013) used a Rapid-Scan Doppler on Wheels (RSDOW) to collect nearly in-situ radar data of a tornado at near-ground levels as low as 4 m above the ground [68]. They used a combination of radar and anemometer data to examine the wind velocity in and near the tornado, and a ground-based velocity-track display (GBVTD) analysis [77] was performed to retrieve the components of the flow. In that tornado, at least, the maximum Vt was found to be at the lowest altitude for which there were data (~5 m height).

A collection of maximum Vt profiles, following the GBVTD analysis, and their elevations are presented in [69] from a few volumes of data from the EF2 Goshen tornado and the F4 Spencer tornado. Specific Vt and Vr at lower altitudes, for example in the case of the Spencer tornado 62 m/s at an altitude of 40 m above the ground, were used for comparison with physical simulation results using the tornado simulator at Western University (WU). Following these comparisons, a scaling match was made for the different scenarios. This is one such example of using near-ground measurements to improve upon existing modelling methods. Unfortunately, not many data sets exist to make this comparison, and as more data becomes available the modelling will improve. Until that happens, mathematical models are often required. Such models are typically calibrated in such a way that the model results closely resemble that of velocity components and structure of tornadoes that occur in nature. Additionally, mathematical models employ simplifications for ease of calculation, which can result in deficiencies in certain aspects of the model as discussed at depth in [73]. It is of note that with all of the limitations of mathematical modelling there is room for more research in this field, and other aspects of tornadoes (e.g., debris flight) can be investigated using this method [72].

A more recent avenue of interest for determining wind speeds near the ground uses tree-fall patterns [78,79,80,74]. Karstens et al (2013) used aerial photographs from the Joplin Tornado and

a tornado that affected Tuscaloosa and Birmingham, Alabama, in 2011 to evaluate simulations of tornadoes [74]. They compared tree-fall patterns associated with analytical simulations of tornadoes passing through forested areas with the observed tree fall patterns to infer tornado structure that produced tree fall behavior most closely matching the observations. Previous approaches involved running the simulation many times until the pattern was subjectively (i.e., visually) close to the observed pattern, but their revised method sought to increase efficiency by establishing this new tree-fall perpendicular orientation criteria. After each run of the simulation was complete, they compared the final results of the simulation to the observed imagery and adjusted the vortex characteristics to improve the agreement between the simulation and observations. They found that the Vt/Vr ratio was much lower than expected.

5. PRESSURE FIELDS IN TORNADOES

There are very few direct pressure measurements in tornadoes owing to the difficultly in purposefully placing instruments in tornadoes and to the violent nature of the winds that may destroy existing instruments. Using mobile radar data and assuming a vortex model, however, one can estimate the pressure perturbation using a GBVTD analysis of the radar-measured data, as Lee and Wurman (2005) did for the Mulhall tornado [64]. The pressure deficit profiles for the Mulhall tornado at different times at an altitude of 50 m are shown in Fig. 8. The pressure inside the tornado core is lower than that in the outer region, as expected, and the lowest pressure occurs at tornado center. The pressure deficit within 800 m of the tornado center is characterized by a smooth yet nonlinear curve towards its maximum deficit of 8400 Pa [64]. Historical pressure deficits in other previous tornadoes are presented in Table 2; they range from 500 to 19200 Pa [59].

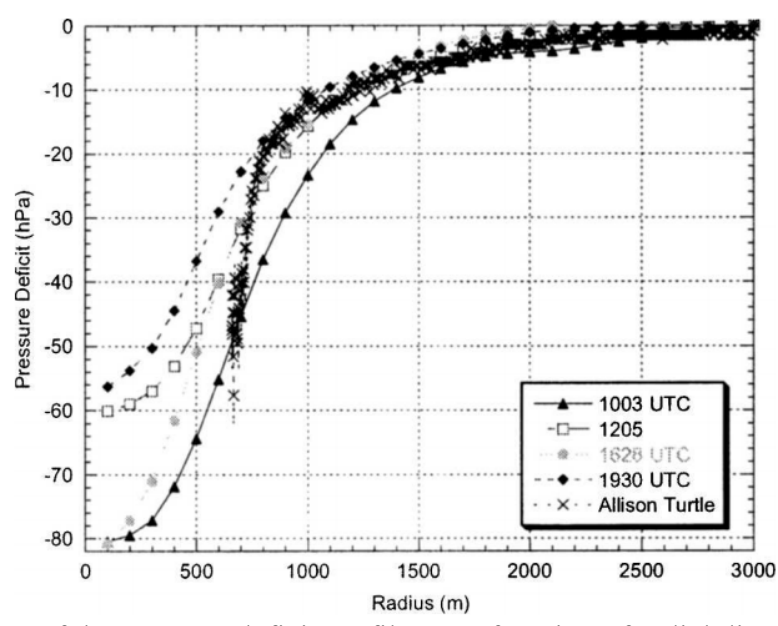


Fig. 8: Comparison of the pressure deficit profiles as a function of radial distance from tornado center from the Mulhall tornado and the Allison, TX tornado in 1995. © American Meteorological Society. Used with permission. [64]

Table 2: Observed Pressure Deficits for Tornadoes from 1894 to 2008 [59, 81].

| Date (Day Month Year) | | Time | Location | Observed Pressure Deficit (Pa) | |
|--------------------------|----------|------|----------|--------------------------------|-------|
| 3 | October | 1894 | 0228 | Little Rock, AR | 1300 |
| 28 | May | 1896 | 0018 | St. Louis, MO | 8200 |
| 21 | August | 1904 | 0345 | Minneapolis, MN | 19200 |
| 25 | June | 1951 | 2130 | Sydney, NE | 1600 |
| 21 | July | 1951 | 0300 | Minneapolis, MN | 1400 |
| 22 | March | 1952 | 2030 | Dyersburg, TN | 2200 |
| 9 | June | 1953 | 0200 | Cleveland, OH | 800 |
| 21 | June | 1957 | 0040 | Fargo, ND | 1200 |
| 10 | May | 1959 | 2120 | Austin, TX | 500 |
| 25 | May | 1962 | 0030 | Newton, KS | 3400 |
| 9 | June | 1966 | 0100 | Topeka, KS | 2100 |
| | | | | Oklahoma City, | |
| 30 | April | 1970 | 0723 | OK | 800 |
| 12 | May | 1970 | 0235 | Lubbock, TX | 1200 |
| 15 | December | 1971 | 0525 | Springfield, MO | 1200 |
| 9 | June | 1995 | 0100 | Allison, TX | 6000 |
| 8 | May | 2002 | 0000 | Mullinville, KS | 2200 |
| 15 | May | 2003 | 2300 | Stratford, TX | 4100 |
| 24 | June | 2003 | 0046 | Manchester, SD | 10000 |
| 24 | June | 2003 | 0050 | Manchester, SD | 5400 |
| 11 | June | 2004 | 1923 | Webb, IA | 2600 |
| 22 | April | 2007 | 0054 | Tulia, TX | 19400 |
| 11 | May | 2008 | 0033 | Broken Bow, OK | 500 |
| 23 | May | 2008 | 2144 | Quinter, KS | 1400 |
| 30 | May | 2008 | 0122 | Tipton, KS | 1500 |
| 30 | May | 2008 | 0217 | Beloit, KS | 1300 |

To understand the pressure distribution in a tornado in a controlled environment, Snow et al. (1980) examined one-celled and two-celled tornado-like vortices generated in a laboratory tornado simulator, and the pressure deficit profile as a function of the radial distance is shown in Fig. 9 [82]. Although the pressure in the core region is much lower than that outside the core for both cases, one-celled vortices have a larger radial pressure gradient in the tornado core than what is seen in the two-celled vortices; the one-celled vortices are characterized by a sharp slope versus a relatively flat profile inside the tornado core of the two-celled vortices. That is, in a one-celled vortex, the lowest pressure is located exactly at the tornado center (Fig. 9a-d), while in a two-celled vortex the tornado core has a relatively broad region of low pressure with small variations (Fig. 9e-g).

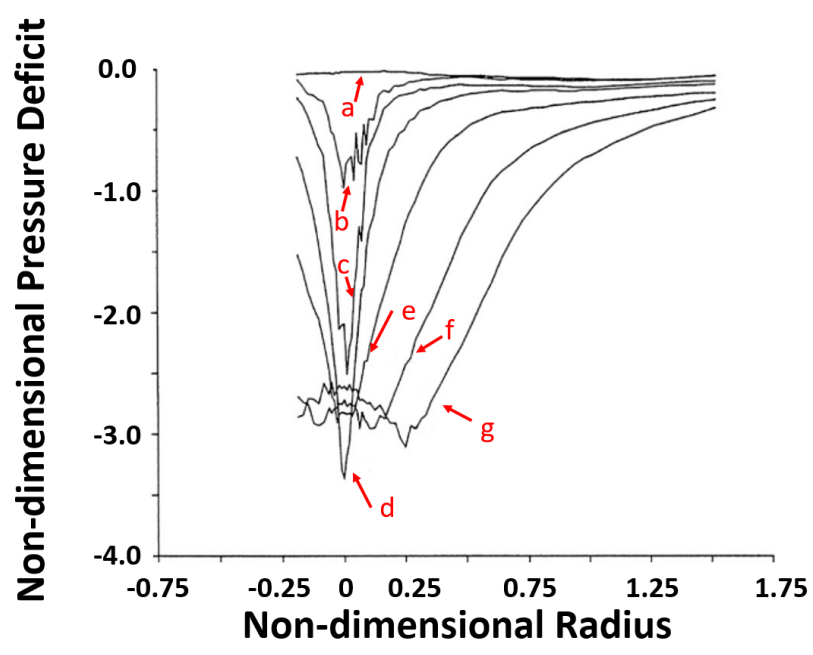


Fig. 9: Laboratory resulted profiles of pressure deficit vs radial distance from tornado center for cases of one-celled vortices, a-d, and two-celled vortices, e-g. © American Meteorological Society. Used with permission. Adapted from Snow et al. (1980) [82].

Karstens et al. (2010) present the measured pressure deficit profiles of some other real-world tornadoes as shown in Fig. 10. The maximum pressure deficit corresponds to the time when the tornado center passes over or nearest to the probes [59]. Based on the observations in Fig. 9, the tornadoes related to Fig. 10b-e may be one-celled tornadoes and the others may be two-celled tornadoes.

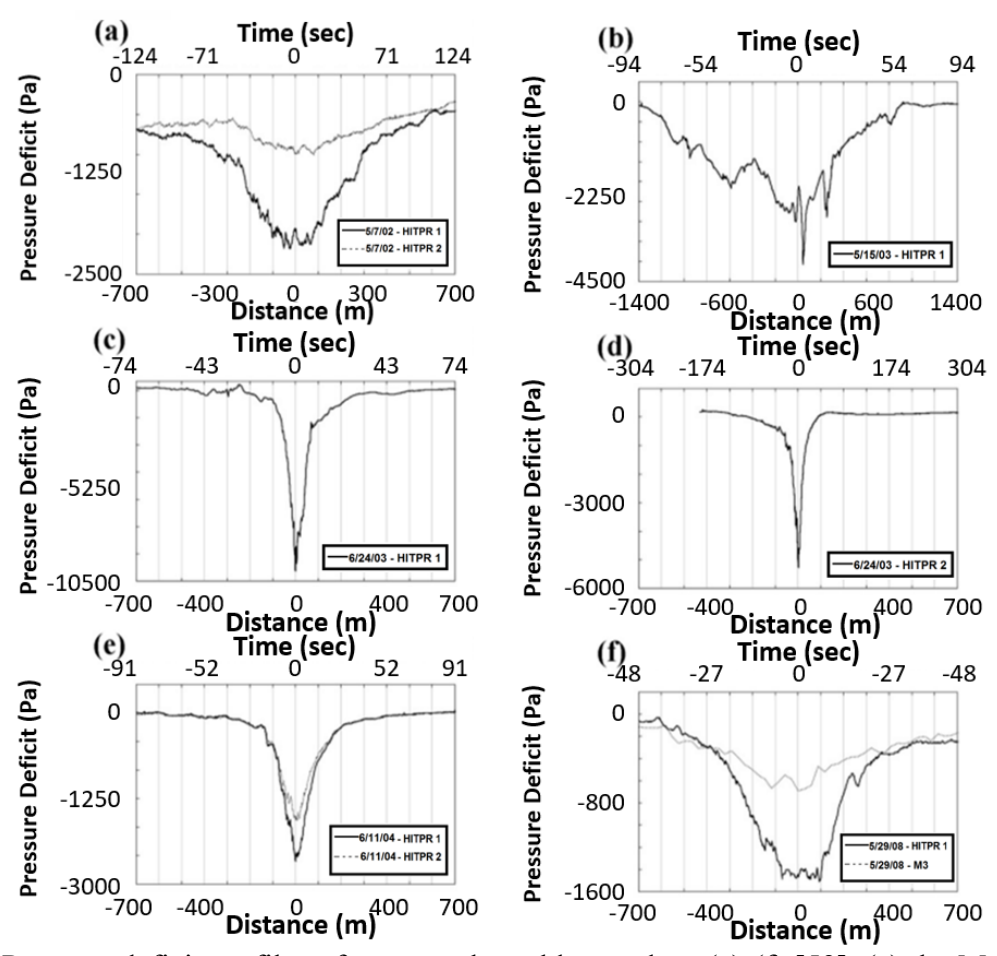


Fig. 10: Pressure deficit profiles of some real-world tornadoes (a)-(f) [59]. (a) the Mullinville, KS tornado on 7 May 2002; (b) the Stratford, TX Tornado on 15 May 2013; (c) the Manchester, SD Tornado on 24 June 2003 (at 0046 UTC); (d) the Manchester, SD Tornado on 24 June 2003 (at 0050 UTC); (e) the Webb, IA Tornado on 11 June 2004; (f) the Tipton, KS Tornado on 29 May 2008. © American Meteorological Society. Used with permission. From Karstens et al. (2010) [59].

6. TORNADO CORE RADIUS

Determining the size of a tornado using meteorological data (e.g., from a radar) is difficult because there is no standard definition for the "edge" of the tornado, and, consequently, measuring the outer "edge" of the tornado with a high level of accuracy is difficult [3, 45]. Even ground-based damage surveys are sometimes unable to determine the "edge" of a tornado (and thus determine its width) because the "edge" of the tornado-produced damage may be ambiguous and inseparable from damage associated with straight-line winds (e.g., from an intense rear-flank downdraft) near the tornado. However, tornado core radius has been well defined and widely used to measure the size of the tornado core. It represents the radius where the maximum tangential velocity is observed. The core radii from several observed tornadoes are shown in Table 3. They range between 50 m and 600 m, though it must be stressed that this is an exceptionally small sample of all tornadoes.

| Table 3: A Small Sample of Tornado Core Radius and Maximum | | | | | | |
|--|------------|-------------------|--|--|--|--|
| Velocity Observed | | | | | | |
| | Tornado | Maximum Doppler | | | | |
| Tornado | Core | Velocity Observed | | | | |
| | Radius (m) | (m/s) | | | | |
| Dimmit, TX on 3 May | 100 | 74 | | | | |
| 1995 [45] | | | | | | |
| Spencer, SD on 30 May | 150 | 100 | | | | |
| 1998 [45] | | | | | | |
| Bridgecreek/ | 175 | Not Available | | | | |
| Moore, OK on 3 May 1999 | | | | | | |
| [18] | | | | | | |
| Oklahoma City, OK on 4 | 200 | 130 | | | | |
| May 1999 [45] | | | | | | |
| Mulhall, OK on 4 May | 600 | 109 | | | | |
| 1999 [45] | | | | | | |
| Hong Kong, China on 6 | 50 | Not Available | | | | |
| September 2004 [52] | | | | | | |
| Goshen County, WY on 5 | 100 | Not Available | | | | |
| June 2009 [48] | | | | | | |

7. FLOW STRUCTURE OF TORNADOES

The structure of the winds within a tornado can vary through the life of any single tornado and from one tornado to the next. Such variability depends on, among other things, the characteristics of the parent convective storm and the environmental (i.e., atmospheric and land) conditions in which the tornadoes occur. In general, the structure of tornadoes can be broadly categorized into two groups: single-vortex and multi-vortex. The single-vortex structure is one in which the vertical vorticity field is dominated by a single maximum near the center of the tornado; single-vortex tornadoes tend to be relatively axisymmetric save for a wavenumber-1 asymmetry associated with translation. Such tornadoes can be further classified into one-celled and two-celled structure [59,83], as shown in Fig. 11.

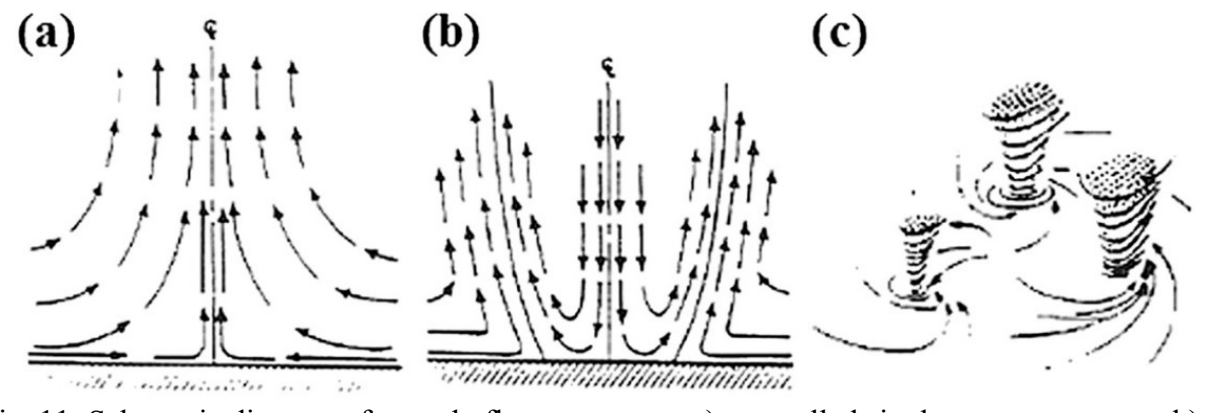


Fig. 11: Schematic diagram of tornado flow structures. a) one-celled single-vortex structure; b) two-celled single-vortex structure c) Structure with multiple vortices. [83]

In a one-celled single-vortex tornado, an updraft is present along the central axis of the tornado; the inflow layer of the tornado is characterized by strong inward-directed flow that turns abruptly upward near the center of the tornado (Fig. 11a). In contrast, in a two-celled single-vortex tornado, a downdraft is present along the central axis, and an updraft is found near the radius of maximum winds (RMW); air within the core region generally flows downward along the central axis, turns outward, and flows upward near the RMW, whereas air outside the core spirals radially inward towards the RMW. Flow within and outside the RMW typically has a non-zero Vt component despite what may be a relatively high Vr component.

A two-celled single-vortex tornado can transition into a multi-vortex tornado owing to shear instability near the RMW. In a multi-vortex tornado, smaller vortices (i.e., "subvortices") rotate around a common center (e.g., Fig. 12), and the strongest winds are usually found within these subvortices. For example, in an intense tornado that occurred near El Reno, OK, on 31 May 2013, Bluestein et al. (2019) reported that radar-measured winds \geq 135 m s⁻¹ were found in a subvortex that was embedded in a broader band of winds characterized by mean radar-measured winds of 80-90 m s⁻¹.

It should be noted that one storm can produce multiple vortices concurrently outside of a multi-vortex tornado. In particular, one or more satellite tornadoes can rotate around an often-larger tornado [Fig. 13a], or concurrent tornadoes can occur as in a "tornado family" (multiple separate tornadoes; Fig. 13b) [18,84,85]. Much more complex behaviors and structures also occur [86]. The wind effects induced by these types of tornadoes on buildings and other structures have not been reported in civil engineering literature. Considering that multi-vortex tornadoes may result in more unfavorable loads to civil structures, the research on multi-vortex tornadoes is reviewed in this section.



Fig. 12: A multi-vortex tornado that occurred on 19 May 2013 in central Oklahoma. At least three subvortices are apparent. (Photo courtesy of Howard Bluestein)



a) A tornado with an associated satellite tornado (small tornado on the left, in 1999 Moore tornado) [87]



b) A Tornado family (produced by a supercell in Nebraska on 16 June 2014) (Photo courtesy of Scott Peake)

Fig. 13: Other situations in which a single storm produces multiple concurrent tornadoes, namely (a) one or more satellite tornadoes that generally rotate around an often larger tornado and (b) a tornado "family", in which multiple separate tornadoes are produced by the same supercell. In the latter case, it is common for one of the tornadoes to be an older, weakening tornado and one to be a newer, developing tornado.

The development of a multi-vortex tornado depends upon two factors – the vortex Reynolds number and wind shear [45,84, 88]. The vortex Reynolds number relates global/environmental rotation to viscosity forces and is defined as [60, 88]

$$Re_{v} = \frac{\Omega L^{2}}{v} = \frac{\Gamma}{v} \tag{1}$$

 Ω = Environmental rotation (rotation of the entire Earth on its axis, which is non-dimensional background rotation)

L = Horizontal length scale of the vertical force

 Γ = Circulation of the system

v =Kinematic viscosity of air

As the vortex Reynolds number increases, the tornado structure changes from a smooth flow to one that has "quasiperiodic oscillations", or flow irregularities [89]. These irregularities are thought to be generated from axisymmetric disturbances. In the laboratory tornado simulator, it is difficult to adjust the vortex Reynolds number due to its reliance on environmental rotation, which is related to the rotation of the earth about its axis [60]. Therefore, the radial Reynolds number is used for convenience. The radial Reynolds number is defined as

$$Re_r = \frac{\rho Q}{\mu h} = \frac{Q}{\nu h} \tag{2}$$

Q = Volume flow rate through the tornado simulator

 ρ = Air density

 μ = Dynamic viscosity of air

h = axial dimension (height of inflow or inlet)

The swirl ratio is also a common metric for determining the structure of a particular tornado. The swirl ratio is defined by [90] as

$$S = \frac{r_0 \Gamma}{2Qh}$$

where r_0 is the radial dimension of the updraft or outlet. In essence, S is a measure of rotational to radial flow. Small values of S (i.e., less than ~ 0.5 but above ~ 0.1) are usually associated with one-celled vortices, and larger values of S (i.e., greater than ~ 0.5) are typically associated with two-celled and multi-vortex tornadoes [91].

The multi-vortex structure of the 2013 El Reno tornado has been studied in more detail by Bluestein et al (2018; 2019) [5]. Traditionally, the analysis of individual subvortices that comprise a multi-vortex tornado is difficult owing to the small size of the subvortices relative to the resolution volume of the radar, the short time scales that characterize subvortices (often of order 1-10 s), and the very fast speeds at which subvortices may move. In this case, the close proximity of the radar to the tornado provided sufficient resolution to identify individual subvortices, and the rapid-scan nature of the radar allowed them to sample the tornado quickly enough to track individual subvortices without aliasing. In this particular tornado, during only the ~2 min period examined, 24 subvortices were identified. The majority of the subvortices developed between 500 m and 750 m from the tornado center, near the RMW of the background flow associated with the tornado. The long-lived subvortices (defined as those lasting at least 15 s) generally moved inwards towards the center of the tornado before dissipation, whereas the short-lived subvortices (defined as those lasting less than 15 s) dissipated near the same radius as they developed. The long-lived subvortices, on average, translated at a slightly lower speed than did the short-lived subvortices. They reported that one particularly intense subvortex (associated with maximum radar-measured radial velocity of at least 135 m/s) translated at ~76 m/s [5]. The average duration and translating speed of subvortices in the El Reno tornado are listed in Table 4.

| Table 4: Average Values for Duration and Translating Speed for Subvortices during the El Reno | | | | | | | | | |
|---|----------------------------|---------|-------------|-------|--|--|--|--|--|
| tornado [5]. | | | | | | | | | |
| | Average Duration (seconds) | Average | Translating | Speed | | | | | |
| | | (m/s) | | | | | | | |
| All Subvortices | 18 | 55 | | | | | | | |
| Long-lived Subvortices | 34 | 52 | | | | | | | |
| Short-lived Subvortices | 8 | 56 | | | | | | | |

A satellite tornado differs from a multi-vortex tornado in that a satellite tornado represents a vortex that is distinctly separated from the main vortex and rotates (like a satellite) around the primary tornado. The distance between a satellite tornado and the primary tornado varies from case to case, but it is noticeably larger than that of subvortices in a multi-vortex tornado. Because they are separate tornadoes, satellite tornadoes may be described as having a different EF-scale rating than the primary tornado. Edwards (2014) identified and examine some of the characteristics of 51 satellite tornadoes [85] and found that the satellite tornadoes tended to produce less severe damage (i.e., have a lower EF-scale rating) than the primary tornadoes that were associated with the satellite tornadoes. In addition, of the primary tornadoes that were associated with a satellite tornado, the primary tornadoes were considerably wider and had longer path lengths than the

average tornado. It can be difficult to assign an EF-scale rating to satellite tornadoes, however, but they tend to be short-lived and may cross the damage path associated with the primary tornado.

Although many think of the condensation funnel when thinking of tornadoes, it is important to remain cognizant of the fact that a tornado's wind field can extend far beyond any visual condensation funnel as indicated in Fig. 14 [92,93]. This funnel is driven by the pressure reduction in the tornado, and the necessary pressure drop needed to produce condensation is affected by the ambient moisture characteristics (i.e., the relative humidity of the air). In an environment with low relative humidity, a very high pressure reduction may be needed to produce saturation and condensation, in which case a weak tornado may not produce any visual condensation funnel. Because of this, photographs or video of a tornado may give misleading information about the size of the tornadic wind field.

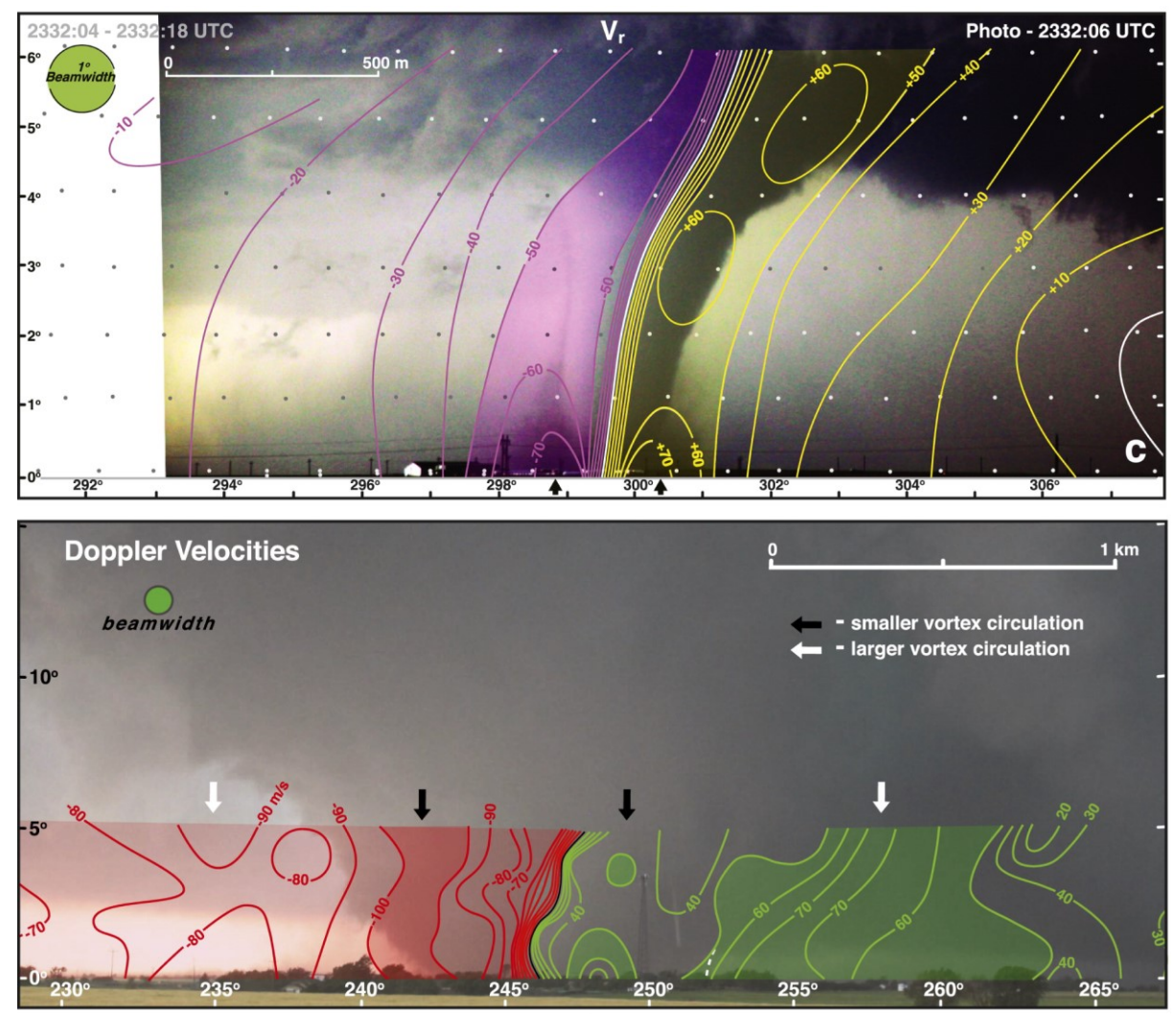


Fig. 14. The Doppler radar-measured velocity fields (contoured and shaded) atop photographs of the (top) 24 May 2016 tornado near Dodge City, KS, and (bottom) the 2013 El Reno tornado. Figure adapted from Wakimoto et al. (2015, 2018). The radar data are valid along a cross-section through the center of each tornado. In both panels, the shading represents velocity magnitudes exceeding 50 m s⁻¹. © American Meteorological Society. Used with permission.

8. RELATIONSHIP BETWEEN DAMAGE, DEBRIS, AND RADAR-MEASURED VELOCITY DATA

The Enhanced Fujita (EF) Scale has been used by the National Weather Service to rate the intensity of tornadoes since 2007 [94,95]. It uses the observed damage from equivalent straight-line wind to infer a wind speed in a tornado; the wind speed estimate is that for a 3-second gust at 10 m AGL [96]. However, the EF scale relies heavily on expert opinion and post-event damage surveys to estimate tornado intensity and obtain an estimate of wind speeds [48]. The estimate of winds from damage can be quite uncertain. However, as noted before, it can be extremely hard to quantify the uncertainty using meteorological observations because extremely limited observations exist that allow for a direct comparison of winds to damage. Weather radars, as noted earlier, have been one of the best tools available for estimating winds in a tornado, but they are almost never available near building height (~10 m AGL), and they do not measure the wind directly (rather, they measure the speed of scatterers within a volume towards or away from the radar). As a result, it is hard to know if differences between the damage produced by the tornado and the winds estimated using radar are the result of errors in the damage-to-wind speed estimate or are attributable to the nature of the radar estimate (e.g., an average of the movement of objects in the air over some volume and time period often at some height well above 10 m AGL). Perhaps the biggest unknown at this time is the vertical profile of winds in the lowest 10-100 m of the tornado. It is highly likely that this profile varies from tornado to tornado and throughout the life of any single tornado, further complicating the study of the relationship between damage and wind speeds.

Wurman and Alexander (2005) reviewed the damage reports from the Spencer tornado and compared them to radar measurements [51]. They found that the wind speeds in the tornado, in terms of the Fujita scale's ranges, varied as the tornado crossed through the town, as shown in Fig. 15 (different colors correspond to different Fujita Scale values). The velocities from radar measurements showed higher values on the south side of the tornadoes path. These higher radar-measured velocities were consistent with the damage surveys for the south side, while the radar-measured velocity on the north side was not consistent with the damage extent in that area [51]. The overall rating of the tornado was F-4, determined from the worst damage observed.

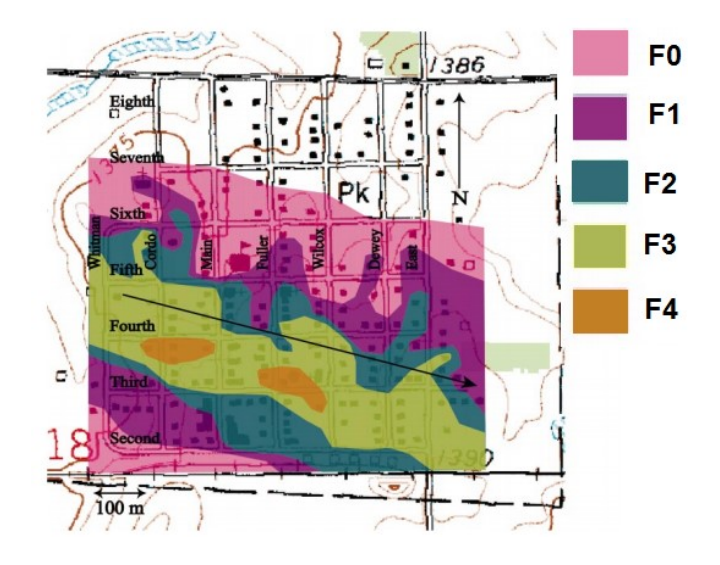


Fig. 15: The Spencer tornado's path through the town of Spencer, SD. © American Meteorological Society. Used with permission. [51]

Based on the above observation, the radar-measured velocity may not be indicative of the true velocity of the air in the tornadic wind field. Snyder and Bluestein (2014) explored the issues involved with comparing radar-measured velocity data to wind speeds as determined by the EF scale [3]. They and others point out that the damage produced during a tornado is not solely reliant upon wind speed and can be attributed to debris type in the wind field, tornado duration, and flow structure of the tornado [3].

Dowell et al (2005) studied the influence of different types of debris in a tornadic vortex on radarmeasured velocities [53]. Two one-dimensional mathematical tornado vortex models (Rankine [66] and Fielder vortex [97]) were applied to four representative types of debris (i.e., small raindrops, large raindrops, large hail/plywood, and bricks), from which relationships between the velocity of the winds and the types of debris (and their densities and concentrations) were established. This was done by adjusting equations that govern object motion and object concentration in a vortex, solving equations for drag force on different types of objects, and using the Rankine and Fielder models as tangential velocity profile assumptions. They found that the obtained relationship correlated with the errors associated with radar measurements because the radar measures the power-weighted mean velocity, not the mean velocity of the actual air molecules, which agrees with the errors presented in radar scanning discussed by Donaldson [98] and Williams et al. [99]. The results are shown in Figs. 16 and 17. The differences between the two models are noted by the sharp turning point of the Rankine model of tangential velocity becoming a curved turning point in the Fielder model. In each case, as the debris becomes larger and denser, the maximum Vt becomes smaller, the tornado core radius becomes greater; the maximum Vr becomes bigger, and the maximum Vw becomes smaller. In addition to these idealized 1-D Vt models, an idealized 2-D model was also employed to identify any other processes that may impact the motion of the objects in a tornado. The 2-D model involved solving equations for motion, drag forces, and vortex flow within a rotating cylinder. These characteristics were then compared to real-world radar measurements from the Spencer tornado. An important point made by Dowell et al (2005) is that the measured data relies heavily upon the debris type and characteristics, and thus the measurements can change as the tornado passes through urban vs rural areas (for which different types of debris are generated).

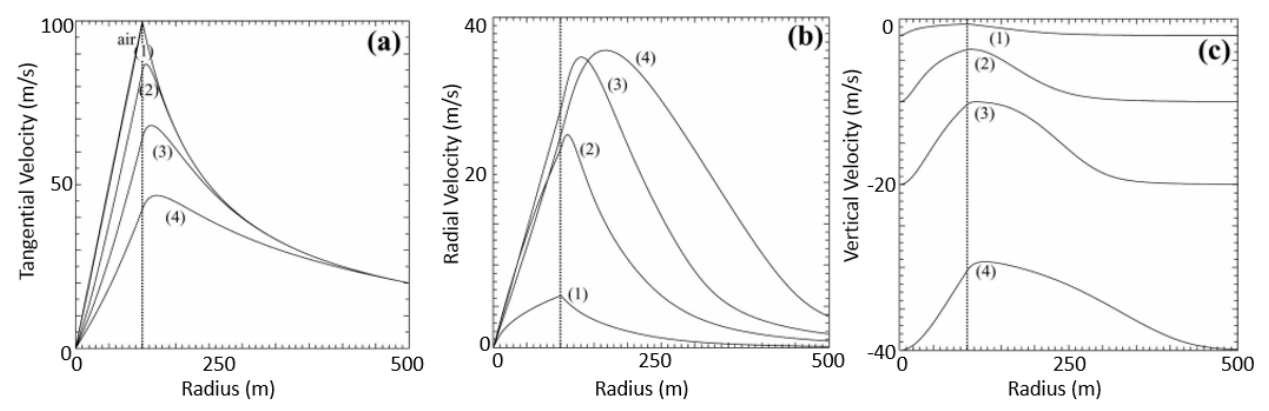


Fig. 16: The tangential, radial, and vertical velocity components with respect to radius found using a Rankine vortex model. 1) Small Raindrops, 2) Large Raindrops/Small Hailstones, 3) Large

Hailstones/Plywood Sheet and 4) Brick. © American Meteorological Society. Used with permission[53]

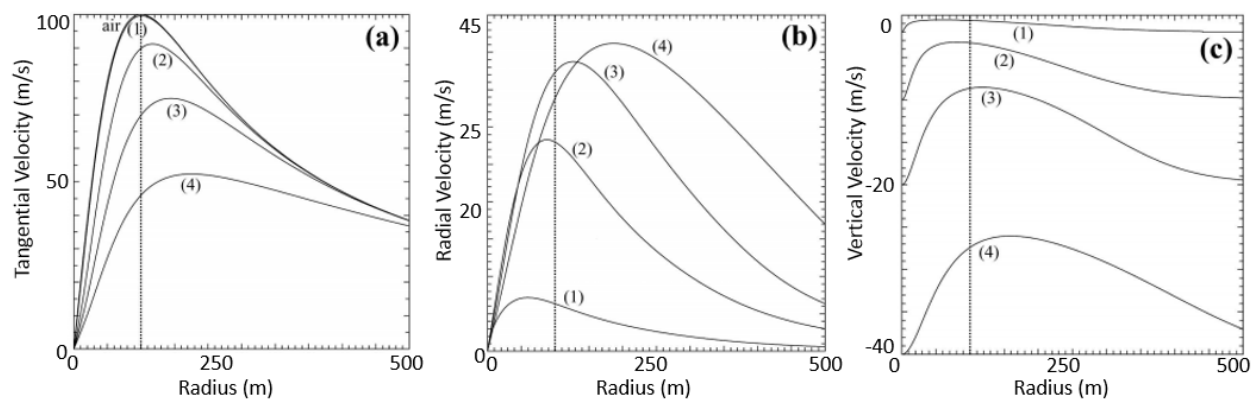


Fig. 17: The tangential, radial, and vertical velocity components with respect to radius found using a Fielder vortex model. 1) Small Raindrops, 2) Large Raindrops/Small Hailstones, 3) Large Hailstones/Plywood Sheet and 4) Brick. © American Meteorological Society. Used with permission. [53]

9. TORNADIC WIND LOAD CALCULATION SPECIFIED IN ASCE7-16

Current design standards for wind engineering (for non-tornadic wind loading) follow the ASCE 7-16 minimum load criteria, outlined in chapter 26 [100]. According to this document, the overall scope is to design the main wind force resisting system (MWFRS) as well as the components and cladding (C&C) to resist wind loads determined using the provisions specified in the ASCE 7-16. Specifically, they define the basic wind speed as a three second gust at 10 m above the ground, straight-line wind speeds. Using this wind speed, the velocity pressure, q, and the structural surface wind pressure, p, on the structure surface, caused by straight-line winds, is determined using the following equations and modifying coefficients. The corresponding coefficients are defined in [100].

$$q = 0.00256K_dK_zK_{zt}K_eV^2 (3)$$

$$p = qGC_p - q_i(GC_{pi}) (4)$$

According to ASCE 7-16, "tornadoes have not been considered in the wind load provisions". There is information in the ASCE 7-16 commentary that provides two methods for minimizing structural damage and improve the safety of occupants, but this is not mandatory. They are the Simplified Method and the Extended Method.

The Extended Method uses Eq. 3 with the design wind speed, V, taken as either the maximum wind speed from the target design EF scale or from the wind speed map in ICC 500, FEMA P-320, or FEMA P-361. The remaining modifying coefficients for Eq. 3 and 4 are determined using an alternate method, described in the ASCE 7-16 commentary, to account for the difference between straight-line and tornadic wind effects. The Simplified Method combines the changed parameters in the Extended Method into a single tornado multiplier, which is intended to make the extended method easier to follow. This is claimed to "achieve the same results" [100]. Unfortunately, some of the coefficients included have been examined by the current authors and the assumptions and simplifications involved in determining them were found to be improper, majorly due to the lack

of field measured pressure/velocity measurements and the related research with regards to civil structures.

10. CHARACTERIZATION OF TORNADIC WIND FIELDS USING CFD SIMULATIONS OR LABORATORY TORNADO SIMULATOR FROM THE FIELD OF METEOROLOGY

Rasmussen et al (1994) stated that, "Scaled-up extrapolations of laboratory measurements to full-scale tornadoes must be viewed with caution [49]." Furthermore, they claim that the use of pre-set boundary conditions leads to uncertainties in calculation and prediction of real-world values and that physical observations of real-world tornadoes provide more useful information for tornado theorists. This ideology supports the use of real-world data over that found in experiment, either numerical or physical. However, the real-world data is difficult to be collected in terms of physical danger and the fleeting nature of tornadoes. Therefore, besides characterizing tornadic wind fields from the field measurements, as reviewed above, tornado researchers in the field of meteorology also characterize tornadic winds using numerical simulations and laboratory tornado simulators.

An early example of the use of numerical modeling of tornadoes is the approach implemented by Lewellen and Lewellen (1996). They discussed the reliance upon boundary conditions to mimic the observed real-world phenomena [101]. A variation that is discussed in their paper is the translation of the tornado. The assumption of axisymmetric flow and constant circulation are applied to the numerical simulation. Additionally, emphasis is put on the swirl ratio. They used a surface boundary condition that had a constant speed of 15 m/s, opposite of the tornado's translation direction, with a horizontal boundary condition that imposed a turbulent surface layer, to mimic translation. Inside the computational domain a 1 km disk, which is used as an outlet surface for the simulation, was placed at a height of 2 km with a uniform updraft velocity of 21.9 m/s. From the simulation, they concluded that the tilt of the vortex are caused by the translation of the simulated vortex. Additionally, tornado center had a 75% lower pressure than the cylindrical region over the upper part of the domain.

The original physical tornado simulator was developed by Ward in 1972 and is known as the Ward-type tornado simulator [102,103]. In this simulator, a central fan was applied to generate a suction updraft in the middle of the simulator, and guide vanes around the convergence chamber (at the bottom) were applied to introduce angular momentum to the air, as shown in Fig. 18. The original Ward-type's primarily use was for meteorological study [91,104].

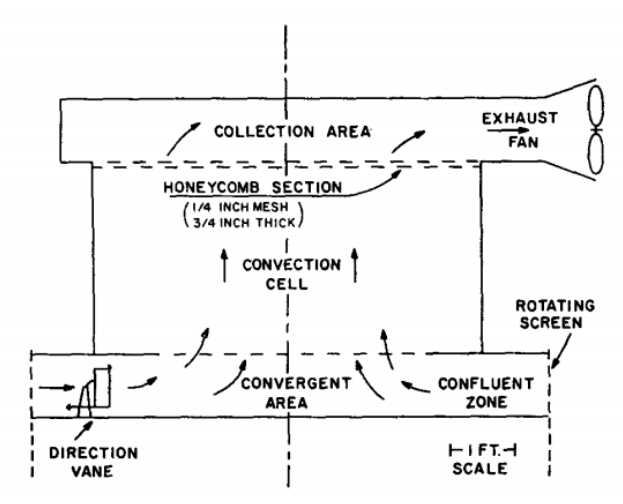


Fig. 18: The original Ward-type tornado simulator developed by Ward in 1972. [103]

Fielder and Rotunno (1986) did testing in a non-translating tornado simulator, as shown in Fig. 19. They observed that the tornado vortex generated by this non-translating laboratory tornado simulator had similar flow structure to the real-world tornado where the vortex makes contact with the ground [105]. From their observation, they believed that the influence of asymmetrical vortexes would be minimal on the wind effects induced on civil structures. However, this belief is up for debate in the field of civil engineering due to the complexities of wind-structure interaction.

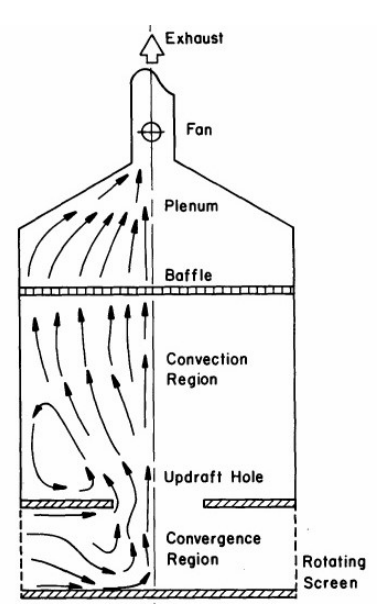


Fig. 19: The basic premise behind the Purdue simulator used by Fielder and Rotunno. © American Meteorological Society. Used with permission. [105].

Dessens (1972) used a tornado simulator, called a vortex cylinder, see Fig. 20, to evaluate the effects of surface roughness on tornadic wind fields [106]. His simulator is composed of a closed cylinder with a fan at the top and a partial hood near the fan, which generated updraft and downdraft within the cylinder. No honeycomb straighteners are mentioned. He used pebbles glued

to a wood plate to simulate surface roughness. He found that the introduction of surface roughness increased the vertical velocity and decreased the tangential velocity.

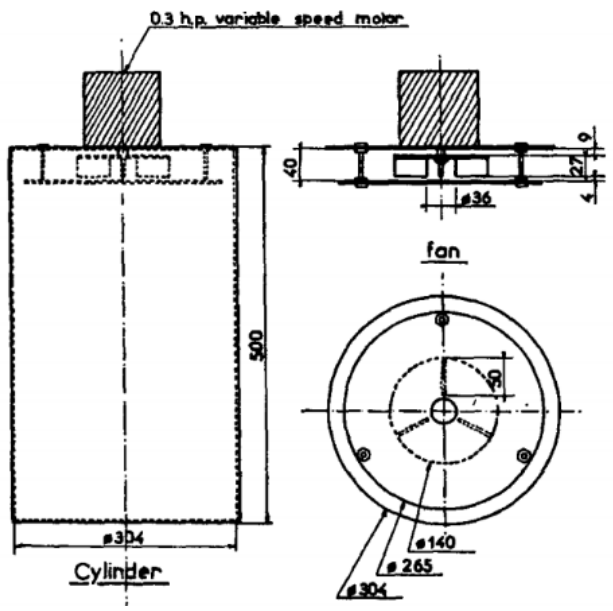


Fig. 20: Dessens' Vortex Cylinder, units are in millimeters. © American Meteorological Society. Used with permission. [106]

Leslie (1977) improved the original Ward type device by moving exhaust duct to above the honeycomb section, to promote axisymmetric flow, and moving exhaust to inside the lab to prevent outside wind from affecting flow with alterations, as shown in Fig. 21 [107]. In order to develop tornado vortices with different swirl ratio and multi-vortex conditions, he introduced surface roughness elements to induce a boundary layer, similar to the atmospheric boundary layer, to generate a flow that was closer to the real-world observations. From his research he found that surface roughness made the flow more turbulent and as the surface roughness increased, the tangential velocity decreased and the vertical and radial velocities increased.

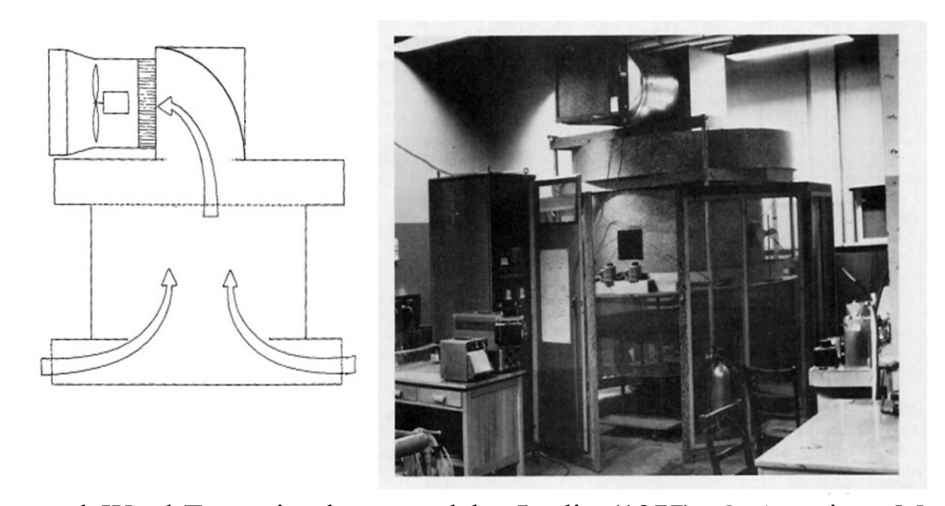
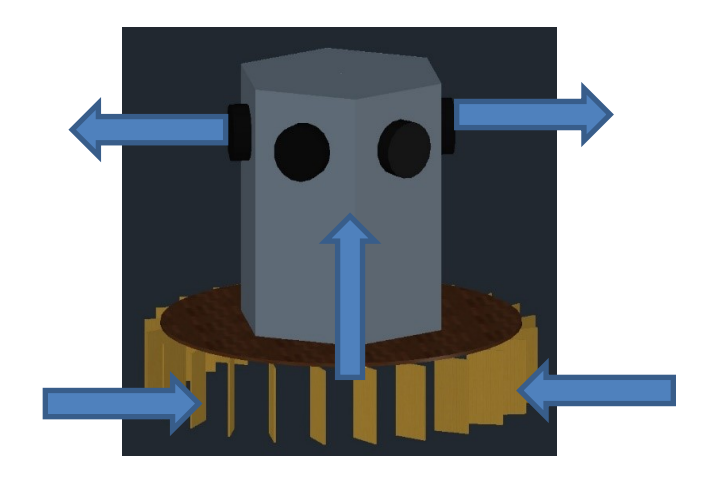


Fig. 21: Improved Ward-Type simulator used by Leslie (1977). © American Meteorological Society. Used with permission. [107].

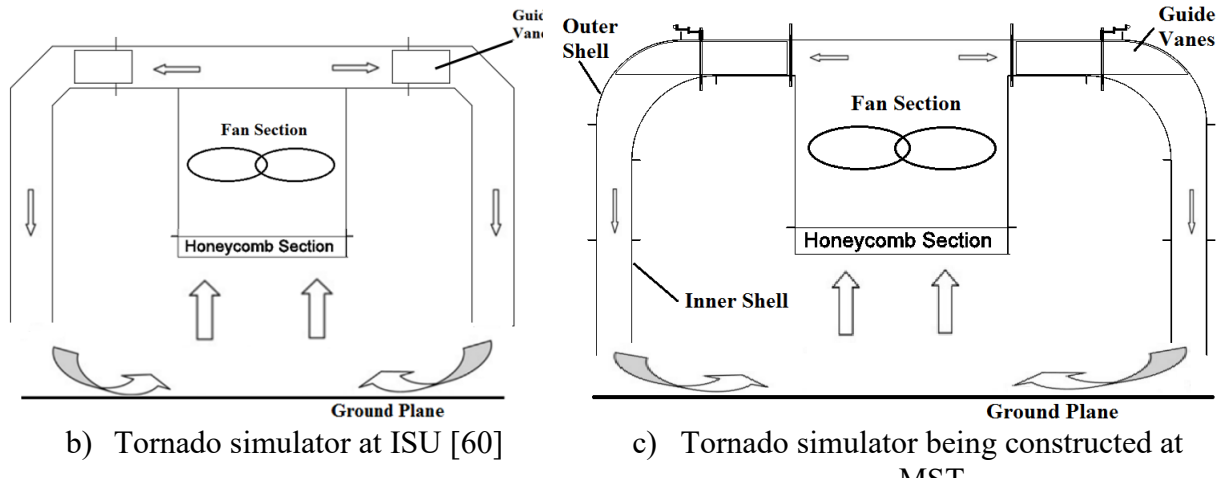
11. CHARACTERIZATION OF TORNADIC WIND FIELDS USING CFD SIMULATIONS OR LABORATORY TORNADO SIMULATOR FROM THE FIELD OF CIVIL ENGINEERING

In order to investigate the wind effects induced by tornadoes on civil structures, researchers in Civil Engineering have been conducting their study through laboratory tornado simulator and numerical simulation. Specifically, research institutions have included physical tornado simulators in their research programs and adapted some knowledge from meteorology into their designs. In recent years, three such laboratory tornado simulators have been built in North America. They are located at Texas Tech University [108], Iowa State University (ISU) [60], and WU [109]. The Texas Tech simulator follows a similar design to that of the Ward-type model, but the size is much larger than any other Ward-type model currently in use, as shown in Fig. 22 (a). The ISU simulator generates its wind field using a central fan, but with recirculating air flow through the duct formed by an outer shell and an inner shell, as shown in Fig. 22 (b) [60]. The simulator at WU has walls of fans surrounding the testing area with a large central fans at the top in the center, serving as the pressure-outlet, as shown in Fig. 22 (d). Tornado simulations are run by turning the fans in the walls to specific angles, to rotate the air as it enters the simulator. In addition to these, another three tornado simulators have been constructed in Asia, one in China, at Tongji University [26], and two in Japan, at Tokyo Polytechnic University (TPU) [27,28] and at the Building Research Institute [29]. Utilizing these simulators, tornadic wind fields have been characterized and their effects on low-rise buildings have been investigated [26,27,28,29,30,31,32,33,34,35,36,37]. Currently, the present authors at Wind Hazard Mitigation Laboratory have designed a laboratory tornado simulator that follows the same mechanism as ISU to generate swirling wind flow. However, they improved the design by adding roundness to the upper ducts and extending the guide vanes through the whole length of the turning section, away from the fan outlet, as show in Fig. 22 (c).

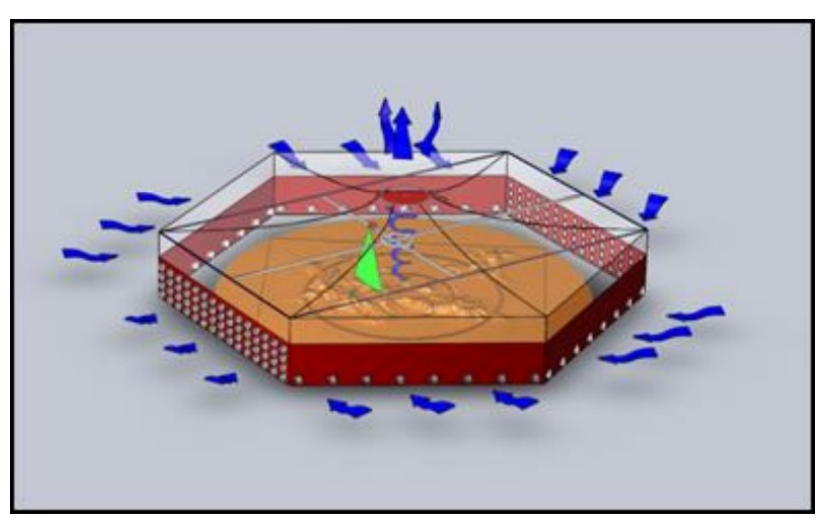




a) Texas Tech tornado Simulator



MST



d) WindEEE (Wind Engineering, Energy, and Environment) at WU [110]

Fig. 22: Three tornado simulators built recently in North America for large-scale testing and one currently being built.

Although CFD simulations have been applied by civil engineering researchers, most CFD simulations were used to validate the generated wind flow in the laboratory tornado simulators. The use of CFD simulations to study tornadic wind effects on civil structures is rare [111,112]. For example, Kuai et al. (2008) modeled the tornado simulator at ISU by using a "sheared inflow initial condition", which is an initial condition possessing tangential and radial velocities with vertical velocity set to zero, at the lower side sections of a cylinder, as shown in Fig. 23 [61]. Additionally, an outlet, located where the bottom of the fan is in the physical simulator, was set to have a vertical velocity, with tangential and radial velocity set to zero. The velocity input at the velocity inlet follows the tangential and radial velocity extracted from radar-measured data. No mechanical components were modeled in their numerical model. They further simulated the flow field of a full-scale tornado to verify the capabilities of their model and found that their results were comparable, but not completely accurate at that scale.

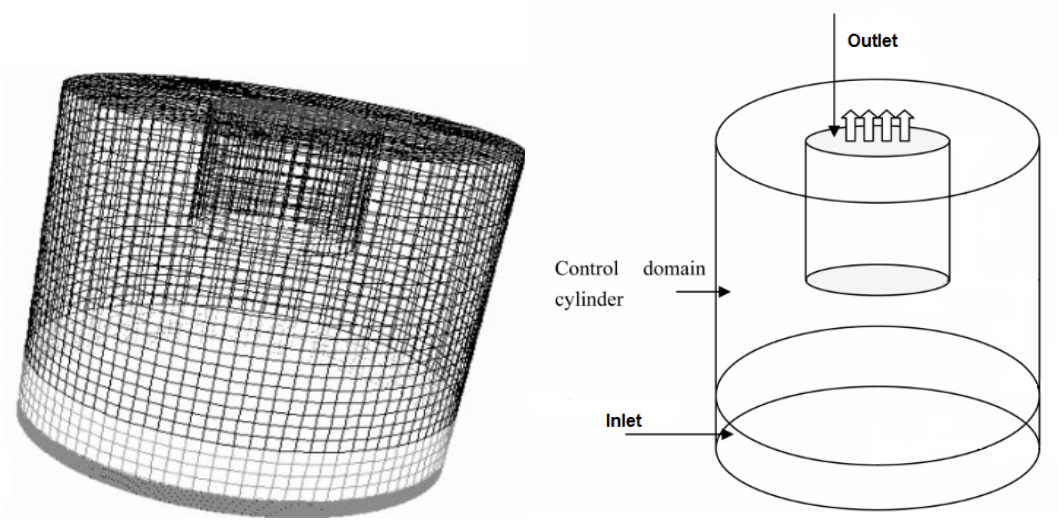


Fig. 23: Numerical model of the ISU simulator developed by Kuai, et al. [61]. a) Computational domain and b) Boundary condition setup

Cao et al. (2018) developed a numerical model of their laboratory tornado simulator, which followed the same principles as the ISU simulator [113]. Rather than replicate the full mechanical sections of their simulator, they simplified their modeling by removing the guide vanes, fan, and upper ducts and replacing them with a velocity inlet, at the bottom of the lower duct opening, and pressure outlets, where the simulator is open to air and at the location where the top of the fan is located in the physical simulator, shown in Fig. 24. But they did apply a porous media effect to the pressure outlet at the bottom of the fan. At the velocity inlet, they applied tangential and radial velocities. They compared their results to the Mulhall and Spencer tornadoes and found acceptable agreement with their results.

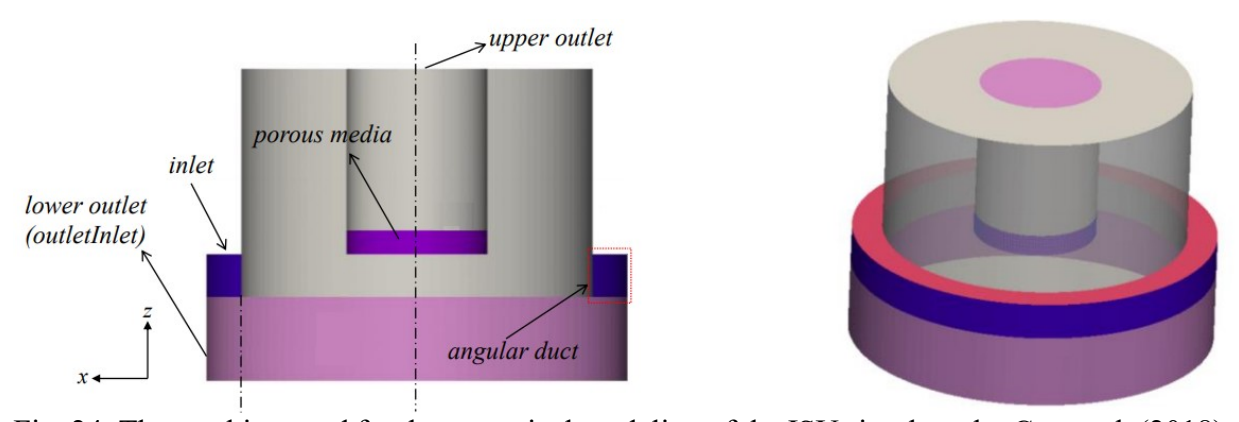


Fig. 24: The meshing used for the numerical modeling of the ISU simulator by Cao et al. (2018). The velocity inlet replaces the descending duct in the physical simulator, an upper outlet replaces the fan outlet at top of the physical simulator, and a lower outlet replaces the open air section of the lower part of the physical simulator. [113]

Yuan et al (2018) improved previous numerical simulations for an ISU-type tornado simulator by including guide vanes and all the mechanical components in the simulation [114], as shown in Fig. 25. To be specific, they modeled the fan using a fan boundary condition, which applied a pressure jump that is the same as the physical fan, and did not incorporate a velocity inlet or pressure outlet.

This replicates the fan section more realistically. Additionally, they used a porous media boundary condition at the bottom of the fan section to model the honeycomb air straighteners. In all, the wind field generated in their simulation is driven exclusively by the fan boundary condition, which resembles the physical simulator better than other previous numerical simulations.

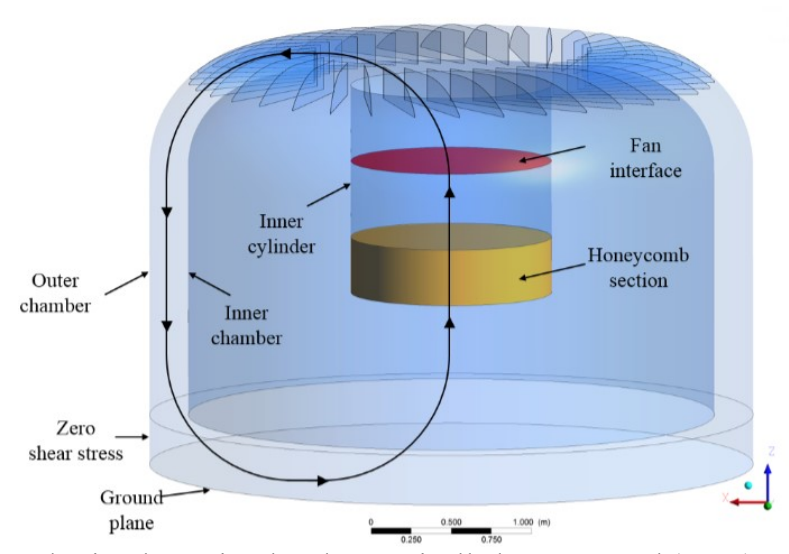


Fig. 25: The tornado simulator simulated numerically by Yuan et al (2018). The system is driven exclusively by the fan boundary condition. [114]

Besides the numerical simulation of the ISU-type simulator, Ishihara et al. (2011) numerically modeled a Ward-type tornado simulator using Large Eddy Simulation as the turbulence model [115]. In their simulation, they modeled the fan as a velocity outlet boundary condition at the top of the computational domain, rather than modeling the fan itself. However, they did model the guide vanes and the honeycomb section. Natarajan (2011) simulated three different tornado simulators using the FLUENT software: the Ward-type, the WindEEE device at WU, and the Atmospheric Vortex Engine [116]. In his model of the Ward-type, he did not model the mechanical components and used an outlet boundary condition instead of a fan where the fan would be in a physical simulator. He compared these results to real-world data and found a comparable agreement.

12. CONCLUSIONS AND FUTURE WORK

To mitigate losses and encourage accurate modeling and research in the field of civil engineering, applied to civil structure design and code improvement, a comprehensive review of field measurements, lab simulations and CFD (computational fluid dynamics) simulations of tornadoes from meteorology has been conducted. From this review, several key tornadoes have been explored and their characteristics have been presented. Specifically, characteristics of these tornadoes have been provided in the following form: velocity in the wind field, pressure distribution in the wind field, tornado core radius, translating speed, and flow structure (single vortex versus multi-vortex; for single vortex, one-celled versus two-celled). Also, information has been reviewed in terms of the driving forces behind tornadoes, and relationships between damage and reported intensity. In addition, physical and numerical study of tornadoes conducted in civil engineering has also been briefly reviewed. The goal of the present authors is to enhance the accuracy of simulation of

tornadic wind fields in civil engineering research by providing the field-measured data from meteorology. This will eventually benefit individual safety, community resilience, and awareness.

To reduce the devastating impact of tornadoes on communities, more robust, tornado-resistant designs for civil structures are needed, and this requires that the effects of winds within tornadoes on civil structures be characterized accurately. To achieve this ultimate goal, researchers in the field of civil engineering have been conducting simulations of tornadic wind fields in laboratory tornado simulators and numerical simulations. The authors have provided a cursory review of the current state of the science from the meteorological perspective, characterizing tornadoes in terms of the velocity components, pressure, tornado core radius, translating speed, and tornado flow structure from several tornadoes analyzed in the literature. In addition, different approaches to simulate tornadic wind fields, physical and numerical simulations, from both the fields of meteorology and civil engineering were reviewed. It is noted that this review was not exhaustive. More papers exist than are reviewed here from the fields of meteorology and civil engineering, but they may not be directly pertinent to this subject.

From this review, it is evident that even though a large amount of information is known with regards to tornado behavior at high above ground ranges, there is little known with regards to near-ground, which is needed for properly determining design tornadic wind loading. The current state of civil engineering to prevent disasters relies heavily upon simulated wind effects found using laboratory tornado simulators and numerical simulations. Despite all the previous research effort, a tornado resistant design has not yet been achieved. To accomplish this ultimate goal, the following research is suggested.

- 1) Characterize the wind fields of tornadoes with multiple vortices. Simulations for single-vortex tornadoes have been widely conducted and reported. However, in reality, most of previous deadly/costly tornadoes possessed multiple vortices. The simulation of this type of tornado has not been sufficiently reported, presumably owing to the computational expense associated with the need to go from a 2-D to a 3-D domain. Research is needed to assess which parameters control the number of vortices in the wind field and properly simulate this type of tornado numerically and in a laboratory, as well as characterize the wind field of this type of tornado.
- 2) Investigate the wind effects on civil structures induced by tornadoes with multiple vortices using numerical and physical experimentation. Since tornadoes with multiple vortices have resulted in significant property loss and fatalities, to really mitigate these losses, it is important to understand the pressure, forces/moments (wind effects) induced by this type of tornado on civil structures. Parametric study may be needed to investigate that influence of the size of civil structures and the size of each vortex on wind effects.
- 3) Investigate the dynamic impact of tornadoes. Although the static impact of tornadoes has been widely studied, the dynamic impact has been rarely studied. This lacking of this information may affect the proper determination of the design tornadic wind loads in terms of gust factor. Therefore, research is need to investigate the non-stationary characteristics of wind effects and the dynamic responses of civil structures.
- 4) Investigate the influence of communities or multiple buildings on tornadic wind fields and wind effects. Currently, when investigating the wind effects on a civil structure, only the structure of interest is placed in the tornadic wind field, ignoring the influence of the presence of the surrounding civil structures on the wind effects of the structure of interest. In order to

properly determine the wind effects on a civil structure, especially for a civil structure located in a city with complicated environment, the surrounding structures should be modelled in the computational domain. Based on this, the characteristics of wind field can be properly captured and the wind effects on the civil structure can be properly determined. Further study can be conducted to determine whether a certain pattern of building layouts increases or decreases the failure rates of the civil structure of interest.

- 5) Two-way coupled numerical simulation considering tornado-structure interaction for flexible structures. Currently, it is assumed that the civil structures in the tornadic wind field is rigid and the civil structures do not deform and thus do not affect the wind field; Therefore, the wind pressure on structural surface obtained from CFD simulations can be simply applied on the finite element model of the civil structures as external loads for structural analysis. This may be true for relatively stiff civil structures. However, for relatively flexible civil structures, this assumption may lead to distorted results. Therefore, research is needed to investigate how two-way coupling can be efficiently achieved between CFD simulations (for wind field) and finite element analysis (for structural analysis) under tornadic winds and how different the obtained wind effects by using two-way coupled simulations are from those obtained from one-way coupled simulation.
- 6) Properly determine design tornadic wind loads by modifying the pressure equation in ASCE 7-16 to calculate the wind pressure on structural surface. To be specific, the coefficients in the pressure equation need to be modified by comparing the wind effects induced by the tornadic wind field and the equivalent straight-line wind field, since the pressure equation specified in ASCE7-16 is based on straight-line winds. Therefore, systematic comparison of wind effects on civil structures under tornadic winds and straight-line winds may be need.

ACKNOWLEDGMENTS

The authors greatly appreciate the financial support from National Science Foundation, through the following two projects, "Damage and Instability Detection of Civil Large-scale Space Structures under Operational and Multi-hazard Environments" (Award No.: 1455709), and "Collaborative Research: CoPe EAGER: Coastal Community Resilience Bonds to Enable Coupled Socio-Physical Recovery" (Award No.: 1940192).

REFERENCES

- 1 http://glossary.ametsoc.org/wiki/Tornado
- 2 Bluestein, H. B., Unruh, W. P., LaDue, J., Stein, H., & Speheger, D. (1993). Doppler-radar wind spectra of supercell tornadoes. *Mon. Wea. Rev.*,121, 2200–2221
- 3 Snyder, J. C. & Bluestein, H. B. (2014). Some Considerations for the Use of High-Resolution Mobile Radar Data in Tornado Intensity Determination. *American Meteorological Society: Weather and Forecasting*, 29, 799-827.
- 4 Houser, J. L., Bluestein, H. B., & Snyder, J. C. (2016). A Finescale Radar Examination of the Tornadic Debris Signature and Weak-Echo Reflectivity Band Associated with a Large, Violent Tornado. *American Meteorology Society, Monthly Weather Review*, 144, 4101-4130.
- 5 Bluestein, H. B., Thiem, K. J., Snyder, J. C., & Houser, J. B. (2018). The Multiple-Vortex Structure of the El Reno, Oklahoma, Tornado on 31 May 2013. *American Meteorology Society: Monthly Weather Review*, 146, 2483-2502.

- 6 The National Severe Storms Laboratory of National Oceanic and Atmospheric Administration (NOAA). (http://www.nssl.noaa.gov/education/svrwx101/tornadoes/)
- 7 Grazulis, T.P., & Grazulis, T. P. (1993). Significant Tornadoes, 1680-1991 (p. 825). St. Johnsbury, VT: Environmental Films.
- 8 National Weather Service. (2018). Tornado Awareness. *National Oceanic and Atmospheric Administration* https://weather.gov/cae/tornado.html Accessed Oct. 2018.
- 9 Changnon, S. A. (2009). Tornado losses in the United States. *Natural hazards review*, 10(4), 145-150.
- 10 McCarthy, D., & Schaefer, J. (2004). Tornado Trends over the Past 30 Years. In Preprints, *14th Conf. Applied Climatology*, Seattle, WA, Amer. Meteor. Soc., CD-ROM.
- 11 Storm Prediction Center. (2014). "Storm prediction center WCM page." www.spc.noaa.gov/wcm> (Mar. 20, 2015).
- 12 Simmons, K. M., Sutter, D., & Pielke, R. (2013). Normalized tornado damage in the United States: 1950–2011. *Environmental Hazards*, 12(2), 132-147.
- 13 Brooks, H. E. & Doswell, C. A. (2002). Deaths in the 3 May 1999 Oklahoma City Tornado from a Historical Perspective. *Weather and Forecasting*, 17, 354-361.
- 14 Lott, N., Smith, A., Houston, T., Shein, K., & Crouch, J. (2012). Billion dollar US weather/climate disasters, 1980-2011. National Climatic Data Center (http://www.ncdc.noaa.gov/oa/reports/billionz.html).
- 15 FEMA (2012). Spring 2011 tornadoes: April 25–28 and May 22, Building performance observations, recommendations, and technical guidance. *Mitigation Assessment Team Report, FEMA* P-908, 512. (http://www.fema.gov/library/viewRecord.do?)
- 16 Strader, S. M., Ashley, W., Irizarry, A., & Hall, S. (2015). A climatology of tornado intensity assessments. *Meteorology Applications*, 22, 513-524.
- 17 Huang, Z., Fan, X., Cai, L., & Shi, S.Q. (2016). Tornado hazard for structural engineering. *Natural Hazards*, 83, 1821-1842.
- 18 Wurman, J., Alexander, C., Robinson, P., & Richardson, Y. (2007). Low-Level Winds in Tornadoes and Potential Catastrophic Tornado Impacts in Urban Areas. *Bulletin of the American Meteorological Society*; 31-46.
- 19 Brooks, H.E. and J. Correia. (2018). Long-Term Performance Metrics for National Weather Service Tornado Warnings. *Wea. Forecasting*, 33, 1501–1511, https://doi.org/10.1175/WAF-D-18-0120.1
- 20 Mei, W., Pasquero, C., & Primeau, F. (2012). The effect of translation speed upon the intensity of tropical cyclones over the tropical ocean. *Geophysical Research Letters*, 39, 1-6.
- 21 (2018). Hurricane Forecasting in the United States. *American Meteorological Society (AMS)*. https://www.ametsoc.org/index.cfm/ams/about-ams/ams-statements/statements-of-the-ams-inforce/hurricane-forecasting-in-the-united-states/. Accessed 2 Aug 2018.
- 22 Savory, E., Parke, G. A., Zeinoddini, M., Toy, N., & Disney, P. (2001). Modelling of tornado and microburst-induced wind loading and failure of a lattice transmission tower. *Engineering Structures*, 23(4), 365-375.
- 23 Simmons, K. M., & Sutter, D. (2005). WSR-88D radar, Tornado warnings, and tornado casualties. *Weather and Forecasting*, 20(3), 301-310.
- 24 http://www.spc.noaa.gov/faq/tornado/ef-scale.html
- 25 Kuligowski, E. D., Lombardo, F. T., Phan, L. T., Levitan, M. L., & Jorgensen, D. P. (2014). Final Report, National Institute of Standards and Technology Technical Investigation of the May 22, 2011, Tornado in Joplin, Missouri. *National Institute of Standards and Technology*, 1-494.

- 26 Wang, J., Cao, S., & Cao, J. (2014). Characteristics of wind loads on a cooling tower exposed to the tornado-like flow. *The 2014 World Congress on Advances in Civil, Environmental, and Materials Research (ACEM14)*, Busan, Korea, 1-13.
- 27 Rajasekharan, S. G., Matsui, M., & Tamura, Y. (2013). Characteristics of internal pressures and net local roof wind forces on a building exposed to a tornado-like vortex. *Journal of Wind Engineering and Industrial Aerodynamics*, 112, 52-57.
- 28 Sabareesh, G. R., Matsui, M., & Tamura, Y. (2013). Ground roughness effects on internal pressure characteristics for buildings exposed to tornado-like flow. *Journal of Wind Engineering and Industrial Aerodynamics*, 122, 113-117.
- 29 Kikitsu, H., Sarkar, P.P., & Haan, F.L. (2011). Experimental study on tornado-induced loads of low-rise buildings using a large tornado simulator. *Proceedings of the 13th International Conference on Wind Engineering*.
- 30 Hu, H., Yang, Z., Sarkar, P., & Haan, F. (2011). Characterization of the wind loads and flow fields around a gable-roof building model in tornado-like winds. *Experiments in fluids*, 51(3), 835-851.
- 31 Haan Jr, F. L., Balaramudu, V. K., & Sarkar, P. P. (2009). Tornado-induced wind loads on a low-rise building. *Journal of structural engineering*, 136(1), 106-116.
- 32 Chang, C. C. (1971). Tornado wind effects on buildings and structures with laboratory simulation. *In Proceedings of the Third International Conference on Wind Effects on Buildings and Structures* (pp. 231-240).
- 33 Bienkiewicz, B., & Dudhia, P. (1993, June). Physical modeling of tornado-like flow and tornado effects on building loading. *In Proceeding 7th US National Conference on Wind Engineering* (pp. 95-106).
- 34 Fouts, J. L., James, D. L., & Letchford, C. W. (2003). Pressure distribution on a cubical model in tornado-like flow. *In 11th International Conference on Wind Engineering* (Vol. 10, p. x).
- 35 Mishra, A. R., James, D. L., & Letchford, C. W. (2008). Physical simulation of a single-celled tornado-like vortex, Part B: Wind loading on a cubical model. *Journal of Wind Engineering and Industrial Aerodynamics*, 96(8), 1258-1273.
- 36 Sengupta, A., Haan, F. L., Sarkar, P. P., & Balaramudu, V. (2008). Transient loads on buildings in microburst and tornado winds. *Journal of Wind Engineering and Industrial Aerodynamics*, 96(10), 2173-2187.
- 37 Natarajan, D., & Hangan, H. (2012). Large eddy simulations of translation and surface roughness effects on tornado-like vortices. *Journal of Wind Engineering and Industrial Aerodynamics*, 104, 577-584.
- 38 Davies-Jones, R. & Markowski, P. (2013). Lifting of Ambient Air by Density Currents in Sheared Environments. *J. Atmos. Sci.*, 70, 1204–1215, https://doi.org/10.1175/JAS-D-12-0149.1
- 39 Markowski, P. M., Straka, J. M., & Rasmussen, E. N. (2002). Direct Surface Thermodynamic Observations within the Rear-Flank Downdrafts of Nontornadic and Tornadic Supercells. *Monthly Weather Review*, 130, 1692-1721.
- 40 Wurman, J., Dowell, D., Richardson, Y., Markowski, P., Rasmussen, E., Burgess, D., Wicker, L., & Bluestein, H.B. (2012). The Second Verification of the Origins of Rotation in Tornadoes Experiment: VORTEX2. *Bull. Amer. Meteor. Soc.*, 93, 1147–1170, https://doi.org/10.1175/BAMS-D-11-00010.1
- 41 Markowski, P., Richardson, Y., & Bryan, G. (2014). The Origins of Vortex Sheets in a Simulated Supercell Thunderstorm. *Monthly Weather Review*, 142, 3944-3954.

- 42 Markowski, P. (2019). "How tornadoes form." Markowski Research Group. https://sites.psu.edu/pmarkowski/how-tornadoes-form/. Accessed 10 Oct 2019.
- 43 Schenkman, A.D., Xue, M., & Shapiro, A. (2012). Tornadogenesis in a Simulated Mesovortex within a Mesoscale Convective System. *J. Atmos. Sci.*, 69, 3372–3390,https://doi.org/10.1175/JAS-D-12-038.1
- 44 Roberts, B., Xue, M., Schenkman, A.D., & Dawson, D.T. (2016). The Role of Surface Drag in Tornadogenesis within an Idealized Supercell Simulation. *J. Atmos. Sci.*, 73,3371–3395, https://doi.org/10.1175/JAS-D-15-0332.1
- 45 Wurman, J. (2001). The Multiple-Vortex Structure of a Tornado. *Weather and Forecasting*, 17, 473-505.
- 46 De Lima Nascimento, E., Held, G., & Gomes, A.M. (2014). A Multiple-Vortex Tornado in Southeastern Brazil. *Monthly Weather Review*, 142, 3017-3037.
- 47 Wurman, J., Kosiba, K., Robinson, P., & Marshall, T. (2014). The Role of Multiple-Vortex Tornado Structure in Causing Storm Researcher Fatalities. *Bulletin of the American Meteorological Society*, 31-45.
- 48 Wurman, J., Kosiba, K., & Robinson, P. (2013). In Situ, Doppler radar, and Video Observations of the Interior Structure of a Tornado and the Wind-Damage Relationship. *American Meteorological Society*, 835-846.
- 49 Rasmussen, E.N., Straka, J.M., Davies-Jones, R., Doswell III, C.A., Carr, F.H., Eilts, M.D., & MacGorman, D.R. (1994). Verification of the Origins of Rotation in Tornadoes Experiment: VORTEX. *Bulletin of the American Meteorological Society*, 75, 6, 995-1006.
- 50 Alexander, C.R & Wurman, J. (2005). The 30 May 1998 Spencer, South Dakota, Storm. Part I: The Structural Evolution and Environment of the Tornadoes. *Monthly Weather Review*, 133, 72-96.
- 51 Wurman, J. & Alexander, C.R. (2005). The 30 May 1998 Spencer, South Dakota, Storm. Part II: Comparison of Observed Damage and Radar-Derived Winds in the Tornadoes. *American Meteorological Society, Monthly Weather Review*, 133, 72-96.
- 52 Kosiba, K., Robinson, P., Chan, P.W., & Wurman, J. (2014). Wind Field of a Nonmesocyclone Anticyclonic Tornado Crossing the Hong Kong International Airport. Advances in Meteorology, 2014, 1-7.
- 53 Dowell, D.C., Alexander, C.R., Wurman, J., & Wicker, L.J. (2005). Centrifuging of Hydrometeors and Debris in Tornadoes: Radar-Reflectivity Patters and Wind-Measurement Errors. *American Meteorological Society, Monthly Weather Review*, 133; 1501-1524.
- 54 Bluestein, H.B., Weiss, C.C., French, M.M., Holthaus, E.M., Tanamachi, R.L., Fraiser, S., & Pazmany, A.L. (2007). The Structure of Tornadoes near Attica, Kansas, on 12 May 2004: High-Resolution, Mobile, Doppler Radar Observations. *Mon. Wea. Rev.*, 135, 475–506, https://doi.org/10.1175/MWR3295.1
- 55 Tanamachi, R.L., Bluestein, H.B., Houser, J.B., Frasier, S.J., & Hardwick, K.M. (2012). Mobile, X-band, Polarimetric Doppler Radar Observations of the 4 May 2007 Greensburg, Kansas, Tornadic Supercell. *Mon. Wea. Rev.*, 140, 2103–2125, https://doi.org/10.1175/MWR-D-11-00142.1
- 56 Houser, J.L., Bluestein, H.B., & Snyder, J.C. (2015). Rapid-Scan, Polarimetric, Doppler Radar Observations of Tornadogenesis and Tornado Dissipation in a Tornadic Supercell: The "El Reno, Oklahoma" Storm of 24 May 2011. *Mon. Wea. Rev.*, 143, 2685—2710, https://doi.org/10.1175/MWR-D-14-00253.1

- 57 Blanchard, D.O. (2013). A Comparison of Wind Speed and Forest Damage Associated with Tornadoes in Northern Arizona. *Wea. Forecasting*, 28, 408–417, https://doi.org/10.1175/WAF-D-12-00046.1
- 58 Blair, S., Deroche, D., & Pietrycha, A. (2008). In Situ Observations of the 21 April 2007 Tulia, Texas Tornado. *Electronic Journal of Severe Storms Meteorology*, 3, 1-27.
- 59 Karstens, C., Samaras, T.M., Lee, B.D., Gallus Jr., W.A., & Finley, C.A. (2010). Near-Ground Pressure and Wind Measurements in Tornadoes. *Monthly Weather Review*, 138, 2570-2588.
- 60 Haan, F. L., Sarkar, P. P., & Gallus, W. A. (2008). Design, construction and performance of a large tornado simulator for wind engineering applications. *Engineering Structures*, 30(4), 1146-1159
- 61 Gallus, Jr., W. A., Sarkar, P., Haan, F., Kuai, L., Kardell, R., & Wurman, J. (2004). A translating tornado simulator for engineering tests: comparison of radar, numerical model, and simulator winds. *American Meteorological Society*, 22nd Conference on Severe Local Storms.
- 62 Kuai, L., Haan Jr, F. L., Gallus Jr, W. A., & Sarkar, P. P. (2008). CFD simulations of the flow field of a laboratory-simulated tornado for parameter sensitivity studies and comparison with field measurements. *Wind and Structures*, 11(2), 75-96.
- 63 Lombardo, F. T. (2013). Technical Investigation of the May 22, 2011, Tornado in Joplin, MO Tornado Hazard Characteristics. *NCST Advisory Committee Meeting*, https://www.nist.gov/sites/default/files/documents/2017/05/09/NCSTACmtgDec2013LombardoJoplin.pdf>. Accessed 2 Aug 2018.
- 64 Lee, W. & Wurman, J. (2005). Diagnosed Three-Dimensional Axisymmetric Structure of the Mulhall Tornado on 3 May 1999. *American Meteorological Society, Journal of the Atmospheric Sciences*, 62, 2373-2393.
- 65 Bluestein, H.B., W. Lee, M. Bell, C.C. Weiss, and A.L. Pazmany. (2003). Mobile Doppler Radar Observations of a Tornado in a Supercell near Bassett, Nebraska, on 5 June 1999. Part II: Tornado-Vortex Structure. *Mon. Wea. Rev.*, 131, 2968–2984, https://doi.org/10.1175/1520-0493(2003)131<2968:MDROOA>2.0.CO;2
- 66 Lewellen, D. C., Lewellen, W. S., & Xia, J. (2000). The influence of a local swirl ratio on tornado intensification near the surface. *Journal of the Atmospheric Sciences*, 57(4), 527-544.
- 67 Wood, V.T. & White, L.W. (2013). A Parametric Wind-Pressure Relationship for the Rankine versus Non-Rankine Cyclostrophic Vortices. *Journal of Atmospheric and Oceanic Technology*, 30, 2850-2867.
- 68 Kosiba, K. A. & Wurman, J. (2013). The Three-Dimensional Structure and Evolution of a Tornado Boundary Layer. American Meteorological Society, *Weather and Forecasting*, 28, 1552-1561.
- 69 Refan, M., Hangan, H., & Wurman, J. (2014). Reproducing tornadoes in laboratory using proper scaling. *Journal of Wind Engineering and Industrial Aerodynamics*, 135, 136-148.
- 70 Refan, M. & Hangan, H. (2018). Near surface experimental exploration of tornado vortices. *Journal of Wind and Industrial Aerodynamics*, 175, 120-135.
- 71 Arsen'yev, S. A. (2011). Mathematical modeling of tornadoes and squall storms. *Geoscience Frontiers*, 2(2), 215-221.
- 72 Baker, C. J. & Sterling, M. (2017). Modelling wind fields and debris flight in tornadoes. Journal of Wind Engineering and Industrial Aerodynamics, 168, 312-321.
- 73 Gillmeier, S., Sterling, M., Hemida, H., & Baker, C. J. (2018). A reflection on analytical tornado-like vortex flow field models. Journal of Wind Engineering and Industrial Aerodynamics, 174, 10-27.

- 74 Karstens, C. D., Gallus Jr, W. A., Lee, B. D., & Finley, C. A. (2013). Analysis of Tornado-Induced Tree Fall Using Aerial Photography from the Joplin, Missouri, and Tuscaloosa-Birmingham, Alabama, Tornadoes of 2011. *Journal of Applied Meteorology and Climatology*, 52, 1049-1068.
- 75 Frelich, L. E. & Ostuno, E. J. (2012). Estimating Wind Speeds of Convective Storms from Tree Damage. Electronic Journal of Severe Storms Meteorology, 7(9), 1-19.
- 76 Womble, J. A., Wood, R. L., Mohammadi, M. E. (2018). Multi-Scale Remote Sensing of Tornado Effects. Frontiers in Built Environment, Technology Report, 4, 1-21.
- 77 Lee, W. C., Jou, B. J. D., Chang, P. L., & Deng, S. M. (1999). Tropical cyclone kinematic structure retrieved from single Doppler radar observations. Part I: Interpretation of Doppler velocity patterns and the GBVTD technique. *Mon. Wea. Rev.*, 127, 2419-2439.
- 78 Holland, A. P., A. J. Riordan, and E. C. Franklin. (2006). A simple model for simulating tornado damage in forests. *J. Appl. Meteor. Climatol.*, 45, 1597–1611.
- 79 Bech, J., M. Gaya, M. Aran, F. Figuerola, J. Amaro, and J. Arus. (2009). Tornado damage analysis of a forest area using site survey observations, radar data and a simple vortex model. *Atmos. Res.*, 93, 118–130.
- 80 Beck, V., and N. Dotzek. (2010). Reconstruction of near-surface tornado wind fields from forest damage. *J. Appl. Meteor. Climatol.*, 49, 1517–1537.
- 81 Davies-Jones, R. P., & Kessler, E. (1974). Tornadoes. *Weather and Climate Modification*, W. N. Hess, Ed., John Wiley and Sons, 552–595.
- 82 Snow, J. T., Church, C. R., & Barnhart, B. J. (1980). An investigation of the surface pressure fields beneath simulated tornado cyclones. *Journal of Atmospheric Sciences*, 37, 1013-1026.
- 83 Davies-Jones, R. P. (1986). Tornado Dynamics: Thunderstorm Morphology and Dynamics, Thunderstorms: A Social, Scientific, and Technological Documentary. *University of Oklahoma Press*, 197-236.
- 84 Potts, S.L. & Agee E.M. (2002). Multiple Vortex Phenomena in Thunderstorms and Tornadoes: Three Scales of Multiple Vortices. *21st Conference on Severe Local Storms*.
- 85 Edwards, R. (2014). Characteristics of Supercellular Satellite Tornadoes. 27th AMS Severe Local Storms Conference, 1-11.
- 86 Wurman, J. & Kosiba, K. (2013). Finescale Radar Observations of Tornado and Mesocyclone Structures. *Wea. Forecasting*, 28, 1157–1174, https://doi.org/10.1175/WAF-D-12-00127.1
- 87 National Severe Storms Lab (1999). The Oklahoma City Tornado Producing Supercell. National Oceanic and Atmospheric Administration.

 https://www.nssl.noaa.gov/tools/decision/cases/990503/StormA.html Accessed, 11 Oct. 2018.
- 88 Nolan, D.S. (2012). Three-dimensional instabilities in tornado-like vortices with secondary circulations. *Journal of Fluid Mechanics*, 711, 61-100.
- 89 Nolan, D. S. & Farrell, B. F. (1999). The Structure and Dynamics of Tornado-Like Vortices. *Journal of the Atmospheric Sciences*, 56, 2908-2936.
- 90 Church, C., Snow, J. T., Baker, G. L., & Agee, E. M. (1979). Characteristics of tornado-like vortices as a function of swirl ratio: A laboratory investigation. *Journal of the Atmospheric Sciences*, 36(9), 1755-1776.
- 91 Church, C., Snow, J. T., Baker, G. L., & Agee, E. M. (1979). Characteristics of tornado-like vortices as a function of swirl ratio: A laboratory investigation. *Journal of the Atmospheric Sciences*, 36(9), 1755-1776.
- 92 Wakimoto, R.M., N.T. Atkins, K.M. Butler, H.B. Bluestein, K. Thiem, J. Snyder, and J. Houser. (2015). Photogrammetric Analysis of the 2013 El Reno Tornado Combined with Mobile X-Band

- Polarimetric Radar Data. American Meteorological Society, *Mon. Wea. Rev.*, 143, 2657–2683, https://doi.org/10.1175/MWR-D-15-0034.1
- 93 Wakimoto, R.M., Z. Wienhoff, H.B. Bluestein, and D. Reif. (2018). The Dodge City Tornadoes on 24 May 2016: Damage Survey, Photogrammetric Analysis Combined with Mobile Polarimetric Radar Data. American Meteorological Society, *Mon. Wea. Rev.*, 146, 3735–3771, https://doi.org/10.1175/MWR-D-18-0125.1
- 94 http://www.spc.noaa.gov/faq/tornado/f-scale.html
- 95 K.C. Mehta, J.R. Mcdonald, J. Minor, Tornadic loads on structures, in: Hatsuo Ishizaki, Arthur N.C. Chiu (Eds.), *Proceedings of the Second USA–Japan Research Seminar on Wind Effects on Structures*, University of Tokyo, Tokyo, Japan, 1976, pp. 15–25.
- 96 http://www.spc.noaa.gov/faq/tornado/ef-scale.html
- 97 Fielder, B. H. (1988). Conditions for Laminar Flow in Geophysical Vortices. *Journal of the Atmospheric Sciences*, 46, 252-259.
- 98 Donaldson Jr., R.J. (1964). A Demonstration of Antenna Beam Errors in Radar Reflectivity Patterns. *Journal of Applied Meteorology*, 3, 611-623.
- 99 Williams, C.R., Gage, K.S., Clark, W., & Kucera, P. (2004). Monitoring the Reflectivity Calibration of a Scanning Radar Using a Profiling Radar and a Disdrometer. *Journal of Atmospheric and Oceanic Technology*, 22, 1004-1018.
- 100 ASCE. (2016). ASCE Minimum Design Loads and Associated Criteria for Buildings and Other Structures (ASCE 7-16). American Society of Civil Engineers, 1-889.
- 101 Lewellen, W.S. & Lewellen, D.C. (1996). Large-Eddy Simulation of a Tornado's Interaction with the Surface. *Journal of Atmospheric Sciences*, 54, 5; 581-605.
- 102 Chang, C. C. (1966). First real man made tornado is generated in laboratory cage by space scientists at the catholic University of America. News item of PI of CUA.
- 103 Ward, N. B. (1972). The exploration of certain features of tornado dynamics using a laboratory model. *NOAA, Journal of the Atmospheric Sciences*, 29(6), 1194-1204.
- 104 Diamond, C. J., & Wilkins, E. M. (1984). Translation effects on simulated tornadoes. *Journal of the atmospheric sciences*, 41(17), 2574-2580.
- 105 Fielder, B.H. & Rotunno, R. (1986). A Theory for the Maximum Windspeeds in Tornado-like Vortices. *American Meteorological Society, Journal of the Atmospheric Sciences*, 43, 21; 2328-2340
- 106 Dessens Jr., J. (1972). Influence of Ground Roughness on Tornadoes: A Laboratory Simulation. *American Meteorological Society, Journal of Applied Meteorology*, 11, 72-75.
- 107 Leslie, F. W. (1977). Surface roughness effects on suction vortex formation: A laboratory simulation. *American Meteorological Society, Journal of the Atmospheric Sciences*, 34(7), 1022-1027.
- 108 Mishra, A. R., James, D. L., & Letchford, C. W. (2008). Physical simulation of a single-celled tornado-like vortex, Part A: Flow field characterization. *Journal of Wind Engineering and Industrial Aerodynamics*, 96(8), 1243-1257.
- 109 Refan, M. & Hangan, H. (2016). Characterization of tornado-like flow fields in a new model scale wind testing chamber. *Journal of Wind Engineering and Industrial Aerodynamics*, 151, 107-121.
- 110 Refan, M. (2014). Physical Simulation of Tornado-like Vortices. Western University, PhD Dissertation, 1-197.
- 111 Selvam. R. P. (1985). Application of the Boundary Element Method for Tornado Forces on Buildings. Texas Tech University, PhD Dissertation, 1-72.

- 112 Selvam, R. P. & Gorecki, P. (2012). Effect of tornado size on forces on thin 2D cylinder. 3rd American Association for Wind Engineering Workshop, Hyannis, MA, USA, 1-9.
- 113 Cao, S., Wang, M., Zhu, J., Cao, J., Tamura, T., & Yang, Q. (2018). Numerical investigation of effects of rotating downdraft on tornado-like-vortex characteristics. *Wind and Structures*. 26(3), 115-128.
- 114 Yuan, F., Yan, G., Honerkamp, R., Isaac, K., Zhao, M., & Mao, X. (2018). Numerical Simulation of Laboratory Tornado Simulator that can Produce Translating Tornadic Wind Flow. *Journal of Wind Engineering and Industrial Aerodynamics*, 190, 200-217.
- 115 Ishihara, T., Oh, S., & Tokuyama, Y. (2011). Numerical study on flow fields of tornado-like vortices using the LES turbulence model. *Journal of Wind Engineering and Industrial Aerodynamics*, 99(4), 239-248.
- 116 Natarajan, D. (2011). Numerical simulation of tornado-like vortices (Doctoral dissertation, The University of Western Ontario).